INFORMATION TO USERS

This manuscript has been reproduced from the microfilm master. UMI films the text directly from the original or copy submitted. Thus, some thesis and dissertation copies are in typewriter face, while others may be from any type of computer printer.

The quality of this reproduction is dependent upon the quality of the copy submitted. Broken or indistinct print, colored or poor quality illustrations and photographs, print bleedthrough, substandard margins, and improper alignment can adversely affect reproduction.

In the unlikely event that the author did not send UMI a complete manuscript and there are missing pages, these will be noted. Also, if unauthorized copyright material had to be removed, a note will indicate the deletion.

Oversize materials (e.g., maps, drawings, charts) are reproduced by sectioning the original, beginning at the upper left-hand corner and continuing from left to right in equal sections with small overlaps.

ProQuest Information and Learning
300 North Zeeb Road, Ann Arbor, MI 48106-1346 USA
800-521-0600

HS

STUDIES ON THE BIOLOGY OF THE HUMAN CORONAVIRUS, STRAIN 229E

by Douglas A. Kennedy

Thesis presented to the School of Graduate Studies in partial fulfilment of the requirements for the degree of Ph.D. in Microbiology and Immunology

UNIVERSITY OF OTTAWA
OTTAWA, CANADA, 1977

to Mary Ellen

TABLE OF CONTENTS

ACKNOWLEDGEMENTS

The author wishes to acknowledge the assistance of all those who have contributed during the course of this work. In particular, thanks to my supervisor, Dr. C. M. Johnson-Lussenburg; and to Mr. A. Brunner who gave much help with various technical aspects and with the preparation of diagrams. All the members of the academic and support staff of the Department of Microbiology and Immunology have helped in various ways, as has the staff of the Medical Communications Section.

This work was supported in part by grants from the Medical Research Council of Canada.

LIST OF ILLUSTRATIONS

Figure

Figure

LIST OF TABLES

GENERAL INTRODUCTION

The Coronaviridae are a group of viruses infecting man and a number of animal species. One of the more recently recognized virus families, they were first proposed as a taxonomic group in 1968 (Almeida et al., 1968) on the basis of a distinctive common morphology as revealed by negative staining: the virion appeared as a rounded particle bearing a fringe of club-shaped projections "recalling the solar corona." All possessed essential lipid, were resistant to DNA inhibitors, possessed a low density and replicated by budding into cytoplasmic vesicles. These features were recognized at that time as common to avian infectious bronchitis virus (IBV), mouse hepatitis virus (MHV) and several IBV-like viruses recovered from man (e.g. B814 and 229E); but, since that time, coronavirus-like agents have been described from additional species, causing a variety of clinical conditions. As the importance and prevalence of members of this group became recognized, so too has the literature pertaining to them blossomed, and the reader is referred to several excellent reviews which have appeared in the past few years for aspects and references not covered in detail here (McIntosh, 1974; Tyrrell et al., 1975; Bradburne and Tyrrell, 1971; Monto, 1974).

Members of this viral taxon are widely distributed throughout the animal kingdom and display a variety of tissue tropisms. To date, proven or candidate members have been isolated from humans (human coronavirus, HCV), chickens (avian infectious bronchitis virus, IBV), turkeys (bluecomb disease virus, TBDV), mice (mouse hepatitis virus, MHV), rats (rat coronavirus, RCV and sialodacryoadenitis virus, SDAV), swine (transmissible gastroenteritis virus, TGE and hemagglutinating encephalitis virus, HEV), calves (neonatal calf diarrhea coronavirus, NCDCV) (references in Tyrrell et al., 1975 and McIntosh, 1974) and canines (canine coronavirus, CCV) (Binn et al., 1975; Keenan et al., 1976). Many of the above diseases, affecting commercial livestock, are of serious economic consequence.

In man, coronaviruses are also of economic importance as the cause of a significant proportion of respiratory illnesses (reviewed in Monto, 1974) but in contrast to the variety of organ systems infected by non-human strains, human isolates have so far only been firmly implicated in pathology of the upper respiratory tract. There is, however, reason to believe that this picture of human disease is incomplete, and that coronaviruses may also be implicated in hepatitis, nephritis and gastroenteritis.

Several authors have reported the association of coronavirus-like particles with hepatitis (Zuckerman

et al., 1970; Campion et al., 1971; Ackermann et al., 1974), which is suggestive that these may be (one of the) agents responsible for non-type A, non-type B hepatitis (Prince et al., 1974). Electron microscope examination of kidney specimens from cases of an endemic Balkan neuropathy has led Apostolov et al. (1975) to suggest that this disease is also of coronaviral etiology, while Caul and co-workers (Caul and Clarke, 1975; Caul et al., 1975) may have uncovered a link between gastroenteritis and this viral group. This type of speculation is strengthened by the existence of animal models for hepatitis (MHV) and gastroenteritis (TGE, NCDCV, bluecomb, CCV) while several coronaviruses affect the kidneys (MHV, IBV), although not as a sole symptom.

To date, electron microscopy has played the major role in all of these studies, perhaps not surprisingly in view of the fastidious nature of these agents in culture (e.g. Barinsky, 1967; Bradburne and Tyrrell, 1964; Kapikian et al., 1973).

Several of these diseases may be zoonotic in nature or at least closely related to animal coronaviruses, as Zuckerman et al. (1970) found serological reactivity against MHV in the serum of the hepatitis patient in his study, while Apostolov et al. (1975) correlated the nephritis to an association with swine, and Sharpee and Mebus (1975) have detected neutralizing antibody to NCDCV in human sera, suggesting the presence of this or a

related agent as a cause of human gastroenteritis. Further research may well profit from comparative and cooperative studies between the fields of human and veterinary medicine.

There is also the question of where coronaviruses stand in relation to other virus groups. For a long while considered as aberrant myxoviruses, they have been assigned to their own taxon, but there is some similarity between the corona and oncornavirus groups as well. Morphologically the two groups fall into the same category of large enveloped (RNA) viruses, both contain a single stranded high molecular weight genome of RNA which, on analysis in density gradients, presents a characteristic and very similar picture. This similarity has been noted by Garwes et al. (1975) who proposed that there might be an evolutionary relationship at the base of this resemblance. Perhaps also the avidity of MHV for lymphoid tissues (Hirano and Ruebner, 1965; Barinsky and Dementiev, 1968; Biggart and Ruebner, 1970) may be taken as another point of similarity. Balanced against the common features however is the reported lack of sensitivity of coronaviruses to DNA inhibitors which would imply that the two groups, if related, have diverged in their respective metabolic pathways rather significantly. Many of the details of coronavirus replication are, in any case, still unknown, precluding detailed comparisons with other groups.

Coronaviruses are a fascinating group of pathogens, of considerable importance in human and veterinary

medicine, whose roles and functions are as yet largely unknown. While we have not solved all the riddles which have intrigued us in our association with one member of the group--the human coronavirus, 229E (HCV/229E, Hamre and Procknow, 1966)--we have had success in some of our studies, the results of which are presented in the following sections in the hope that they might provide the tools and the insight for others who are favored to be working in this field.

SCOPE OF THE THESIS

The work described here was done as part of a larger study on the biological, chemical and antigenic properties of coronavirus 229E. Undertaken at the beginning of this study, many of the techniques appropriate to working with this virus had to be established, and the first section of this thesis describes the development of a sensitive and useful plaque assay which has permitted the accurate quantitation of virus necessary to various aspects of the larger programme. Other techniques which we have found useful are presented in appropriate parts of the other sections.

The second section describes the effect of Actinomycin D on 229E growing in L 132 cells. It is similar to the first in that the study was begun as an evaluation of a potential tool for suppressing host functions in the infected cell, but it became of interest in itself, indicating a close relationship between the virus and host which probably precludes the intended use of this drug, although the further exploration of this virus-host relationship may prove to be a fruitful area for further research.

The last chapter describes the isolation and partial characterization of a subviral component from the

virus. This study provided insight into the architecture of the virion as well as another tool for the further characterization of this virus. Related studies are continuing under the direction of Dr. Johnson-Lussenburg, aimed at preparing and characterizing this and other subviral components--which work will, in turn, provide the basis for a more detailed examination of the events which occur during the infectious cycle.

I. DEVELOPMENT OF PLAQUE ASSAY TECHNIQUE

Introduction

Two plaque assays for use with 229E virus have been described in the literature. The first, reported by Hamre et al. in 1967, was for the production of plaques on monolayers of Wl-38 cells. In 1969, Bradburne and Tyrrell noted that the Hamre medium did not appear suited for use with L 132 cells and described the development of another overlay medium for use with these cells. Both of the above assays were performed in petri dishes, requiring the use of CO_2 incubators, but they differed in the composition of the overlay medium and in the method of staining plaques for counting.

As cell culture and virus production in this laboratory was being done in closed containers of L 132 cells, it was considered that a plaquing system which could be used in these same conditions would be expedient. In preliminary experiments, neither of the above overlays was satisfactory. Subsequent experiments led to the development and characterization of another plaquing technique. The relevant experiments are described in this section.

Materials and Methods

i) Virus

Coronavirus strain 229E was obtained from Dr. A. Z. Kapikian at the U.S. National Institutes of Health, Bethesda, Maryland. It was reported as having been passed in Wl-38 cells and was initially carried through two passes in Wl-38 cells in this laboratory. Thereafter it was passaged in L 132 cells.

ii) Cells

The L 132 line, derived from human embryonic lung (Davis and Bolin, 1960) was obtained from Mr. D. A. McLeod, Laboratory Centre for Disease Control (LCDC), National Health and Welfare, Ottawa; who in turn had obtained it from the American Type Culture Collection (ATCC).

The passage number from tissue of origin is unknown (Shannon and Macy, 1972) but our numbering system continues on from that used by LCDC. Prior to receipt in this laboratory they had been passaged five times at a 1 to 2 ratio at LCDC; subsequently they were carried at 1 to 3 split ratios. Cells used in this study were between passage 14 and 55, generally in the lower half of that range.

Wl-38 cells, a diploid cell strain derived from human embryonic lung (Hayflick, 1965) were obtained from the ATCC. HF-26-L and HF-62-L (HFL), similar diploid cell

strains from human embryonic lung were obtained through the courtesy of Mr. P. A. Phipps and Mr. B. MacCulloch of the Ottawa Regional Virus Laboratory, Children's Hospital of Eastern Ontario, Ottawa. These strains were used while in Phase II of their passage history (Hayflick and Moorhead, 1961; Hayflick, 1965).

All cell cultures were grown in Eagle's Minimal Essential Medium (MEM, "Auto-Pow," Flow Laboratories, Inc.) supplemented with 10% FCS and antibiotics (penicillin, 100 u/ml; streptomycin, 100 µg/ml and neomycin, 50 µg/ml). Cultures were grown in 75 cm^2 disposable plastic flasks (Falcon Plastics, Inc.) and used within twenty-four hours of reaching confluence.

iii) Preparation of Overlay Media

Eagle's Minimal Essential Medium (MEM) in Earle's balanced salt solution (EBSS) was obtained from Grand Island Biological Co. as a dry powder. Stocks of liquid concentrate without bicarbonate were prepared at five times the recommended strength and sterilized by membrane filtration.

Medium 199 (M 199) in EBSS was also obtained from Gibco as a dry powder, and stocks were similarly prepared as a five-fold concentrate and filter sterilized. Although the concentrate was slightly turbid even after prolonged stirring, the filtrate was clear and the insoluble residue was considered to be of no consequence, since diluted filtrate was used successfully for cell growth.

Hanks balanced salt solution (HBSS) was prepared as a ten-fold concentrate (Schmidt, 1969) and sterilized by filtration. For use in overlays, 0.5% lactalbumin hydrolysate (LAH, Nutritional Biochemicals Co.) was added to a double strength dilution and the mixture was re-sterilized.

a. Additives

The following stocks were prepared in distilled water and membrane filtered for use with the above media; 5.6% sodium bicarbonate (Fisher Certified Reagent), 1% 5-bromodeoxyuridine (BUdR, Calbiochem), 4% DEAE-dextran (Sigma), 3.0M magnesium chloride (Fisher Certified) and 1% neutral red (Fisher Certified). Additives were stored at $4^{o}C$ prior to use.

b. Antibiotics

A combination of penicillin and streptomycin or of penicillin, streptomycin and neomycin was used in the overlay media. Combined stocks were prepared in distilled, deionized water from powder (Nutritional Biochemical Co. or General Biochemicals) at 100,000 units of penicillin, 100,000 µg of streptomycin and 50,000 µg of neomycin (when used) per ml. The mixture was filter sterilized, dispensed in aliquots and stored frozen. For use, stock antibiotics were added to the media at 1/1000 dilution, achieving final concentrations of 100 u /ml, 100 µg/ml and 50 µg/ml respectively for the three agents. Antibiotics were used in all overlays.

c. Serum

Fetal calf serum (FCS) obtained from Flow Laboratories or Gibco was used in these media, and stored frozen at -20°C until used.

d. Agar

Three preparations were evaluated; Agar #1 and Ionagar #2 from Oxoid, as well as Noble agar from Difco. All were prepared as 1.8% stocks in distilled water and sterilized by autoclaving.

Complete media were prepared from the stocks above, adjusting the amount of water to give the correct concentration of constituents. The liquid and agar portions were kept separate until just before use, when nutrient solution and melted agar, both at 45°C were mixed.

iv) Plaque Assay Procedure

Dilutions of virus were prepared in cell growth medium, at ice bath temperature. 0.33 ml inocula were added to well drained monolayers and allowed to adsorb at room temperature for 1 hour, re-distributing the inoculum over the cell sheet at twenty minute intervals.

At the end of the adsorption period, without removing the inoculum, complete overlay medium at 45°C was added to each flask, 25-30 ml per flask. Medium was poured onto the upper, cell free surface, and when the first signs of gelling were apparent, the flask was inverted so as to allow the overlay to harden in contact with the

monolayer. Once the agar had set, the flasks were incubated at 33°C for plaque development with the agar covered monolayer uppermost.

Results

i) Composition of the Overlay Medium

Various plaquing media were evaluated in a series of preliminary experiments. Among those tried were the two described in the literature, variations on their composition, and several combinations of Medium 199 and various additives. In general, neither the medium described by Hamre et al. (1967) nor that of Bradburne and Tyrrell (1969) was suitable; plaque production was poor or absent under MEM-based overlays, while the monolayer deteriorated under HBSS-LAH media. Plaques were produced, however, under an overlay medium which contained M 199, 0.1% $NaHCO_3$, 100 µg/ml each of BUdR and DEAE-dextran, 2% FCS, 0.3% Ionagar #2 and antibiotics.

Fixation with formaldehyde followed by staining of the cultures with crystal violet, as used by Bradburne and Tyrrell, enabled greater numbers of plaques to be counted than the neutral red technique used by Hamre et al.; in addition, it was more convenient to use. These two factors led to the adoption of fixation and staining as the standard procedure in all subsequent plaque assays.

This new overlay could be used for plaquing 229E in either L 132 cells or a diploid fibroblast line from

human lung (HF-26-L) and equivalent numbers of plaques were produced on cultures of either cell type. Parallel titration of a virus suspension by plaque assay and in tube cultures of L 132 cells indicated that the plaque technique was the more sensitive as one TCD_{50} was equivalent to 3.9 pfu. Thus, taken together these preliminary data suggested that the new medium was potentially suitable for our requirements and further studies were carried out to examine the effects of the various constituents on the assay, resulting in several changes in composition.

a. Bicarbonate

During earlier screenings of candidate overlays, it was noted that media containing 0.2% $NaHCO_3$ maintained a more constant pH than those with 0.1%; therefore we prepared test overlays at various bicarbonate concentrations and used these on cells inoculated from a common virus pool.

In the first experiment, the concentration of $NaHCO_3$ was varied from 0.6 to 0.22% and in the second, was varied from 0.22 to 0.39%. The overlay for these trials was Medium 199 with 2% FCS, 100 µg per ml each of BUdR and DEAE-dextran and 0.4% Ionagar #2. Within each experiment all conditions were kept constant, except for the bicarbonate content of the overlay.

In both of these series, plaque numbers were seen to vary markedly in relation to the concentration of

bicarbonate present (Table 1, Figure 1) with an apparent optimum of 0.2% for maximal plaque numbers. In these experiments some difficulty was encountered in handling these assays due to the fluid nature of the agar. Slippage of the agar did occur, and led to the smearing of plaques or, on occasion, loss of the monolayer; therefore the concentration of Ionagar was increased to 0.6% and used at this level in all subsequent trials. This change did not affect the quantitation of 229E in HFL cells.

Subsequent experiments (3 and 4, Table 1) were done as described above but using the higher agar concentration. No loss of cultures or plaque smearing was incurred due to agar slippage and it was also noted that there was less weeping of medium from the overlay during incubation. Apparent titres were not so affected by suboptimal bicarbonate levels as in the previous series and highest plaque numbers were obtained with 0.22% and 0.17% in experiments 3 and 4 respectively (Table 1, Figure 1). On the basis of these trials, 0.2% was retained as standard in the test medium during further evaluation.

Experiments to be described later led to changes in the overlay formulation: M 199 was retained as the nutrient base, but BUdR was reduced to 50 µg/ml from 100, DEAE-dextran increased from 100 to 200 µg/ml, 2% FCS unchanged, but Oxoid agar #1 at 0.6% was substituted for Ionagar #2 at the same concentration. As bicarbonate levels had influenced plaque numbers in the previous media, a similar

TABLE 1

VARIATION IN PLAQUE NUMBERS WITH BICARBONATE CONCENTRATION IN OVERLAY MEDIUM

Experiment Number	Concentration of Sodium Bicarbonate in Overlay, %						
	0.06	0.11	0.17	0.22	0.28	0.34	0.39
1	<6* (<3%)	103 (45%)	132 (57%)	230 (100%)	N.D.	N.D.	N.D.
2	N.D.	N.D.	N.D.	105 (100%)	89 (85%)	69 (66%)	49 (47%)
3	N.D.	35 (88%)	31 (78%)	40 (100%)	33 (83%)	34 (85%)	N.D.
4	N.D.	87 (84%)	103 (100%)	93 (90%)	87 (84%)	79 (77%)	N.D.

* Each value in this table represents the average plaque count of 2 flasks and numbers in parentheses express the plaque count as a percentage of the maximum count in that group.

N.D. = Not done.

FIGURE 1

Figure 1:- Effect of different bicarbonate concentrations in the overlay medium on the numbers of plaques produced by a constant inoculum of 229E virus in L 132 cells. The medium used in experiments 1 and 2 differed from that used in 3 and 4 only in agar content, but this had a marked effect on the degree of response to bicarbonate in the two media; 0.22% $NaHCO_3$, however, was optimal in both.

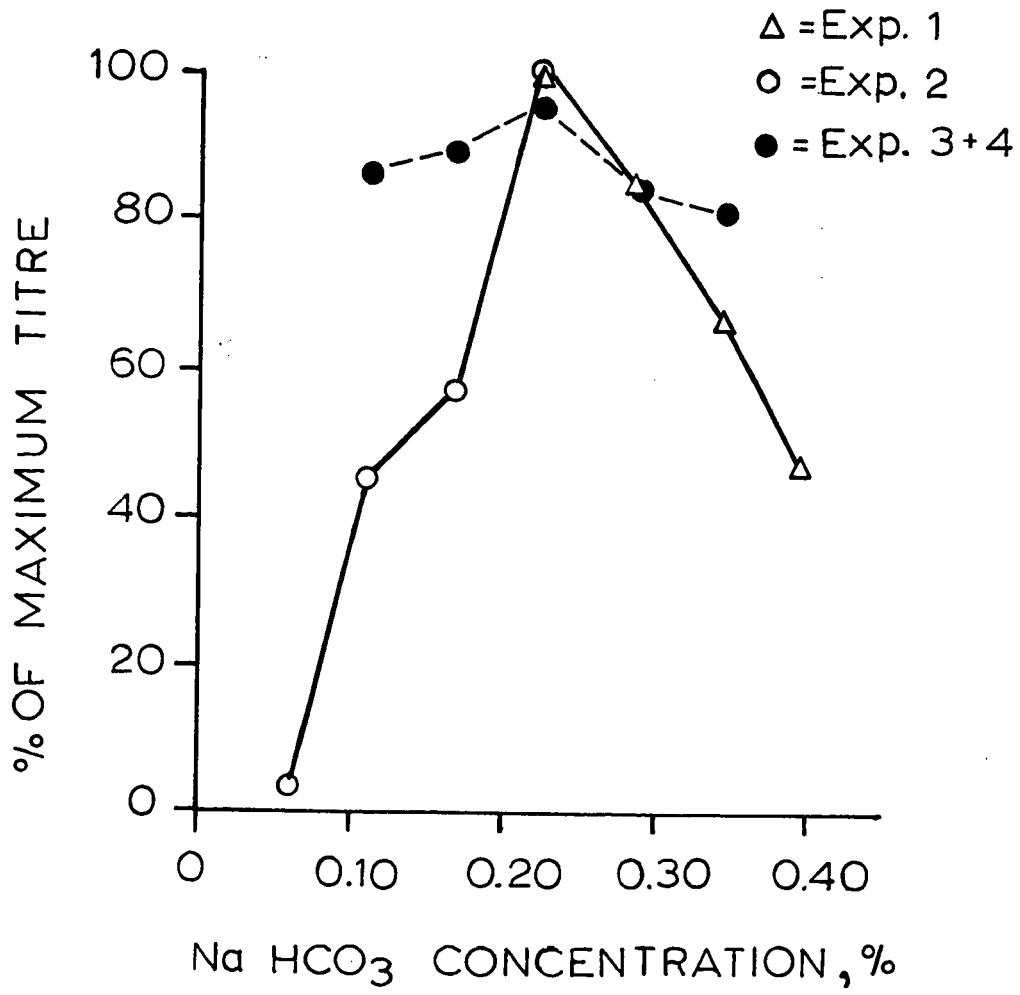
Δ =Exp. 1
○ =Exp. 2
● = Exp. 3+4
100
80
60
40
20
0
% OF MAXIMUM TITRE
0
0.10
0.20
0.30
0.40
Na HCO3 CONCENTRATION, %

determination was done on the new formulation, examining concentrations in the range of 0.1 to 0.3% in steps of 0.05%.

In this new formulation, bicarbonate once again exerted a marked effect on plaque numbers. From the results in Figure 2 it can be seen that similar counts were obtained over the range of 0.1 to 0.2% $NaHCO_3$, then the plating efficiency fell off steeply with further increase in concentration. The plaque morphology also varied in relation to bicarbonate content: the lesions were small at low levels, increasing to a maximum diameter at 0.15 and 0.20% then diminished with further increase in concentration of $NaHCO_3$. Plaque margins were indistinct at the low end of the range and the centres were opaque due to intact cells which had remained attached to the flask. As the content of bicarbonate was increased, the margins became more definite and the centres clearer. In addition to the changes in plaque morphology, the density and uniformity of the cell monolayer also increased with increasing bicarbonate concentration.

Thus, it was concluded that the effect of bicarbonate upon plaque production was considerable, variable and appeared to be affected by changes in the other components of the overlay. A concentration of 0.2% $NaHCO_3$ was optimal or near optimal in all three media in terms of both plaque morphology and numbers and thus it was retained for continued use in the overlay.

FIGURE 2

Figure 2:- Effect of varying bicarbonate content in the final overlay formulation. Concentrations of 0.1-0.2% $NaHCO_3$ permitted the development of equivalent numbers of plaques, but increasing the bicarbonate beyond 0.2% resulted in a sharp drop in plaquing efficiency.

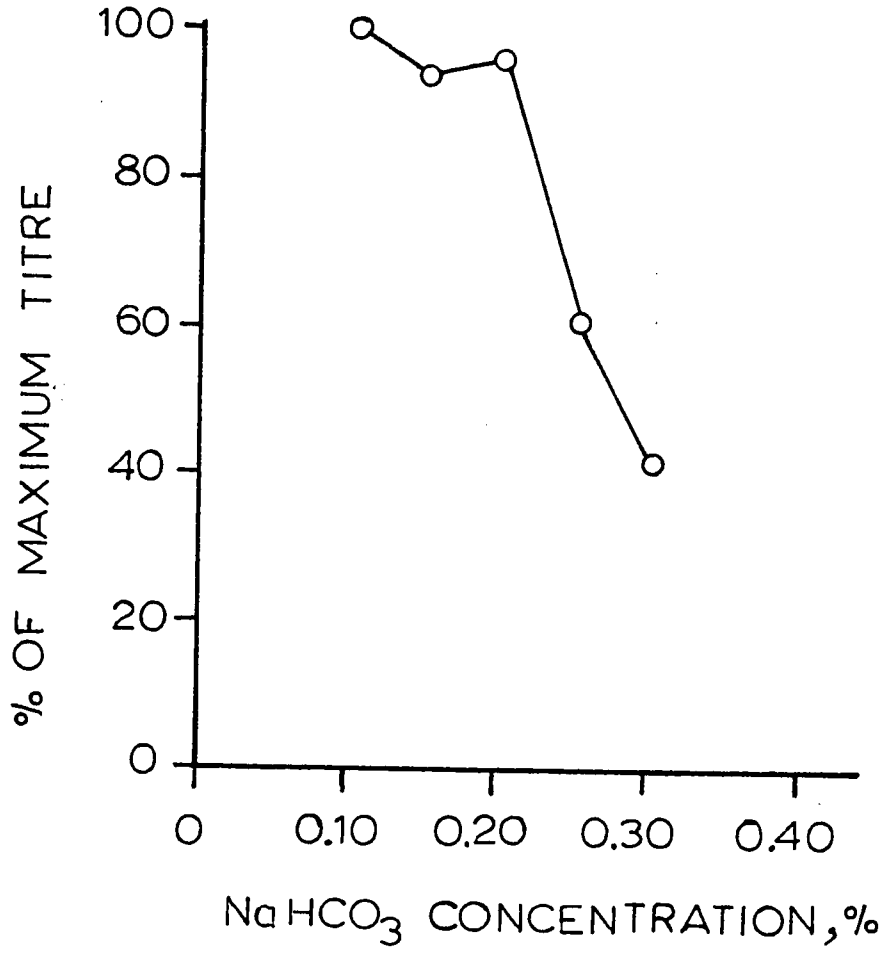
100
80
60
40
20
0
% OF MAXIMUM TITRE
0
0.10
0.20
0.30
0.40
NaHCO3 CONCENTRATION, %

b. Bromodeoxyuridine

Bromodeoxyuridine was a component of the overlay used by Bradburne and Tyrrell (1969) and was also included in our original test overlay. It was now known, however, whether this ingredient was necessary for, or contributed to plaque production in the latter medium. Preliminary studies indicated that omission of both BUdR and DEAE-dextran from the test medium prevented the development of plaques, whereas elimination of BUdR alone led to a marked deterioration in their appearance. This result was confirmed as follows: a series of flasks was inoculated with virus from a common pool. After adsorption, test overlay medium containing various concentrations of BUdR was added and, after incubation, plaques were stained and counted. The resulting plaque numbers were plotted against BUdR concentration (Figure 3). There appeared to be a decline in plaque numbers with increasing concentration of BUdR, but this was not pronounced. However, as can be seen in Figure 4, the size and clarity of the plaques was markedly improved by the presence of 50 µg/ml of BUdR. While there was no further improvement in the plaques at higher concentrations, the thickness and regularity of the cell monolayer diminished at the higher levels.

c. DEAE-dextran

DEAE-dextran, similarly, was present in the overlay of Bradburne and Tyrrell (1969), that of Hamre et al. (1967)

FIGURE 3

Figure 3:- Effect of 5-bromo-deoxyuridine (BUdR) in the overlay medium on the number of plaques produced by a constant inoculum of virus. No striking quantitative effects were manifested over the range examined although there is a suggestion of a slight progressive suppression of plaque production with increasing levels of this additive. Each point represents the average count from two flasks.

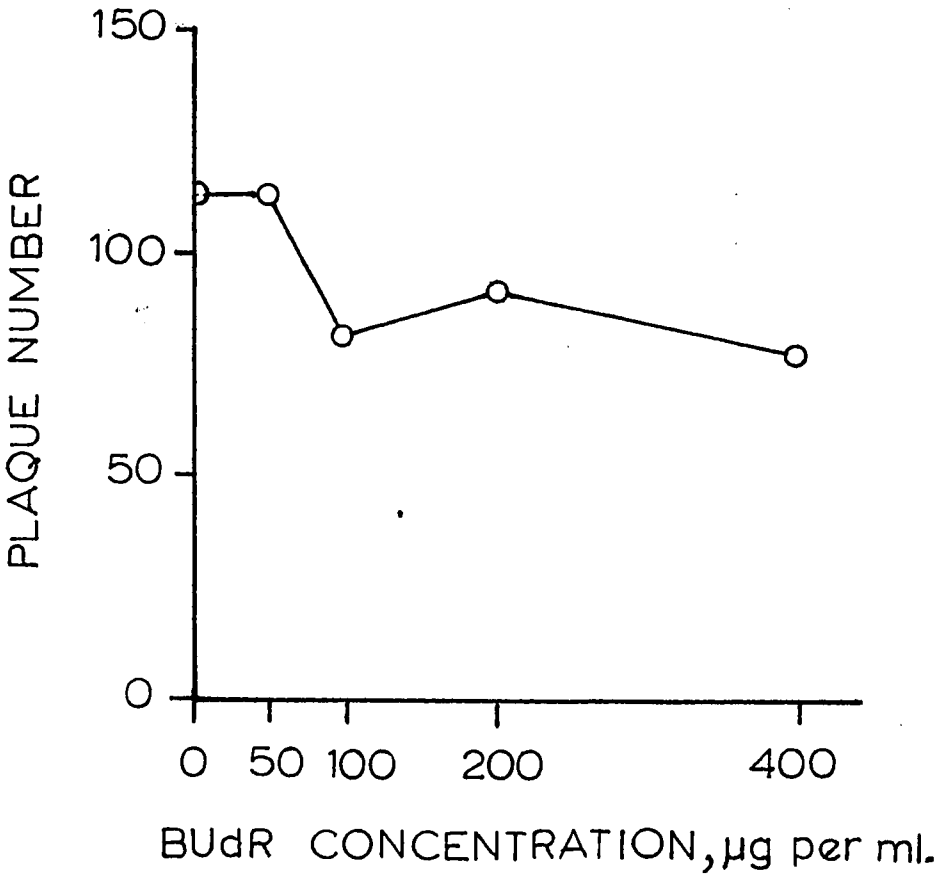
150
100
50
0
PLAQUE NUMBER
0
50
100
200
400
BUdR CONCENTRATION, µg per ml.

FIGURE 4

Figure 4:- Effect of BUdR in the overlay medium on plaque morphology. A. Uninoculated flask of L 132 cells. B-F. Cells inoculated with 229E virus, overlaid with medium containing 0, 50, 100, 200 and 400 µg/ml of BUdR, respectively. Larger and clearer plaques were produced under medium containing BUdR (C-F) but the higher concentrations appeared to adversely affect the cell monolayer. Flasks pictured are from a different experiment from that which produced the data shown in Figure 3.

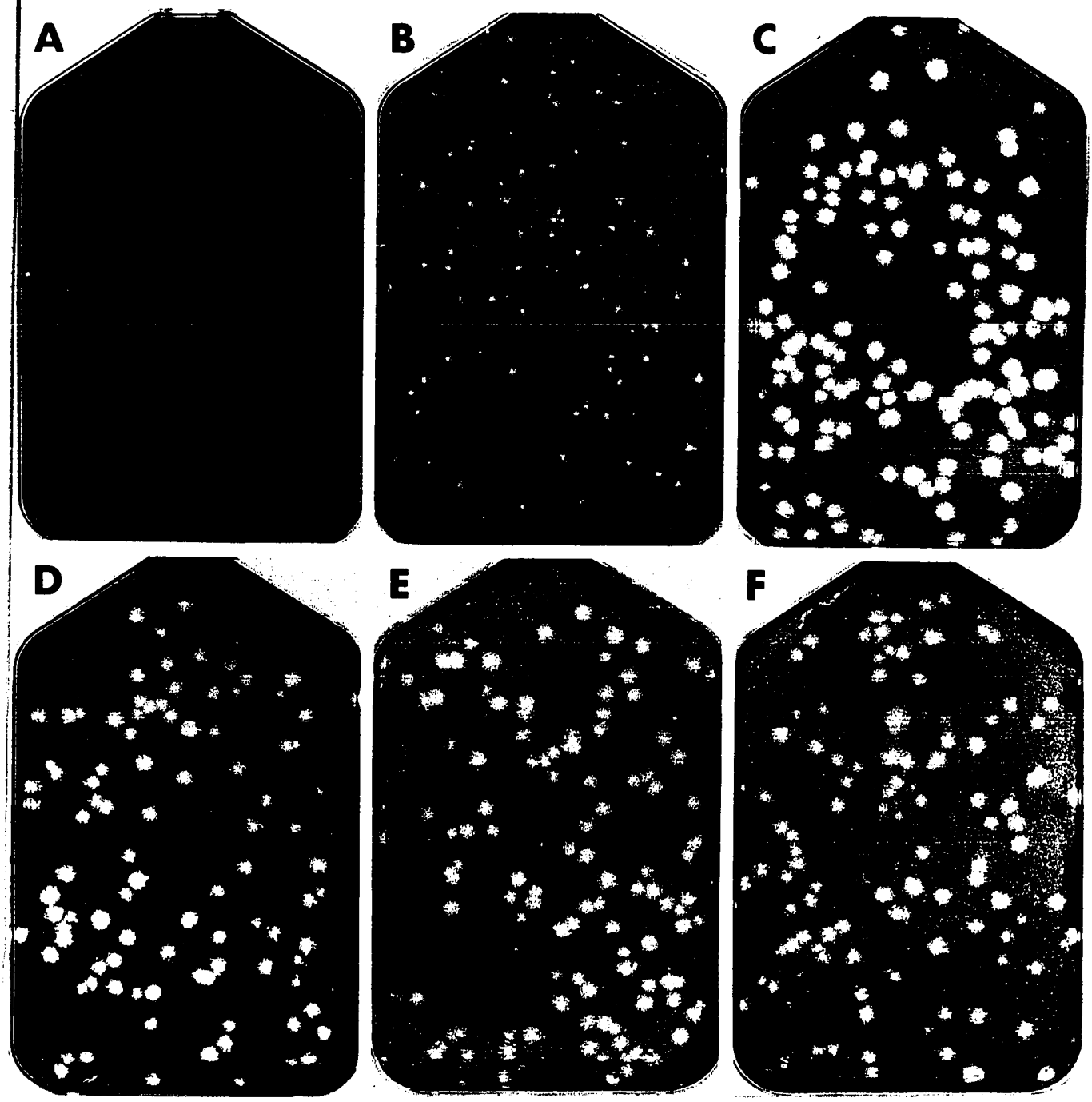
A
B
C
D
E
F

and our own test overlay. To examine its effect in the test overlay a series similar to that done with BUdR was set up with varying concentrations of DEAE-dextran. Although there was no marked variation of plaque numbers with changes in concentration of this additive (Figure 5), plaque size was noted to increase with increasing amounts of this supplement, at least to 200 µg/ml (Figure 6).

d. Magnesium Chloride

Additional $MgCl_2$ was included in the overlay of Bradburne and Tyrrell, however, supplementation of our test overlay with an additional 30 mM $MgCl_2$ did not enhance plaque formation by coronavirus 229E. In one trial overlays with and without extra $MgCl_2$ were compared: both the size of the plaques and the numbers produced were reduced under the supplemented medium (Table 2). The differences were not striking quantitatively, but in any case there appeared to be no reason to increase the $MgCl_2$ content for coronavirus assay. In later work (unpublished), when poliovirus was plaque assayed, an additional 30 mM $MgCl_2$ did enhance plaque formation by this virus (as suggested by Wallis and Melnick, 1962).

e. Agar Preparations

Three purified agar derivatives have been used as solidifying agents in our overlay media, and all allowed plaque development (Table 3). Plaques forming under test medium containing Oxoid Agar #1 were larger, clearer and

FIGURE 5

Figure 5:- Effect of DEAE-dextran in the overlay medium on the number of plaques produced by a constant inoculum of virus. No regular variation in plaque numbers was noted over the range of concentrations examined. Each point represents the average count from two flasks.

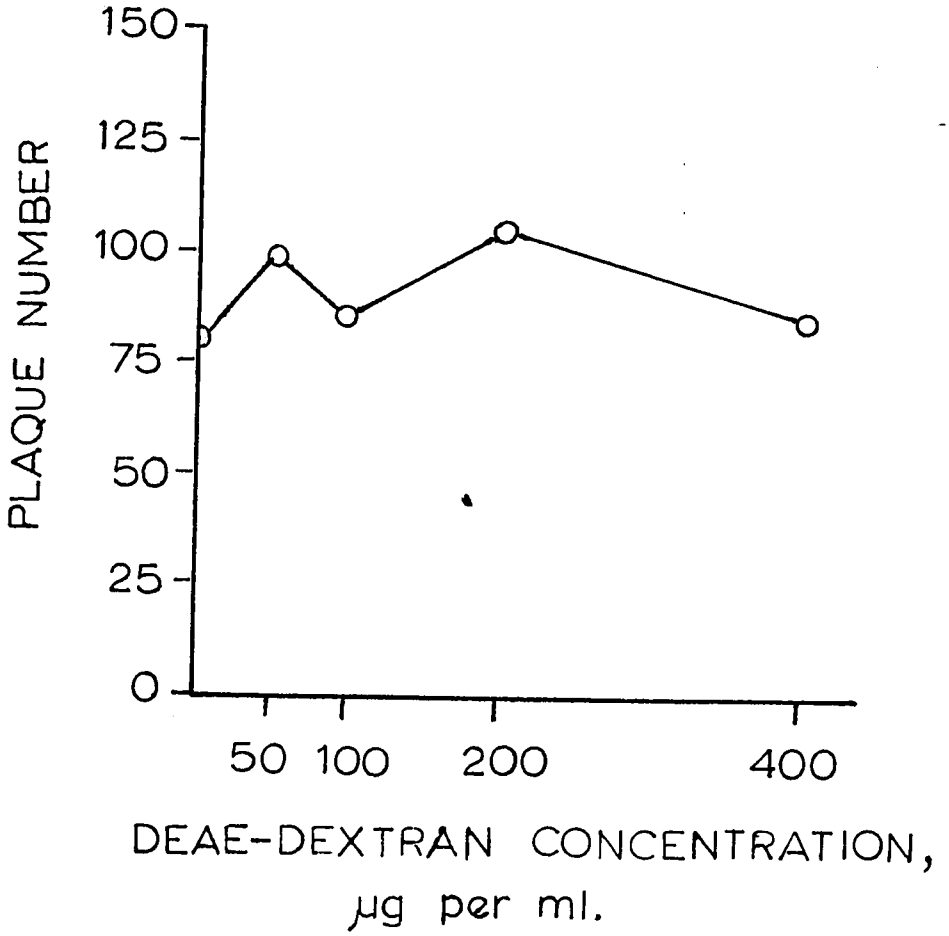
150
125
100
75
50
25
0
PLAQUE NUMBER
50
100
200
400
DEAE-DEXTRAN CONCENTRATION,
μg per ml.

FIGURE 6

Figure 6:- Effect of DEAE-dextran in the overlay medium on plaque morphology. A. Uninoculated flask of L 132 cells. B-F. Cells inoculated with 229E, overlaid with medium containing 0, 50, 100, 200 and 400 µg/ml of DEAE-dextran, respectively. Plaque size was noted to increase with increasing amounts of this supplement, at least to 200 µg/ml (E).

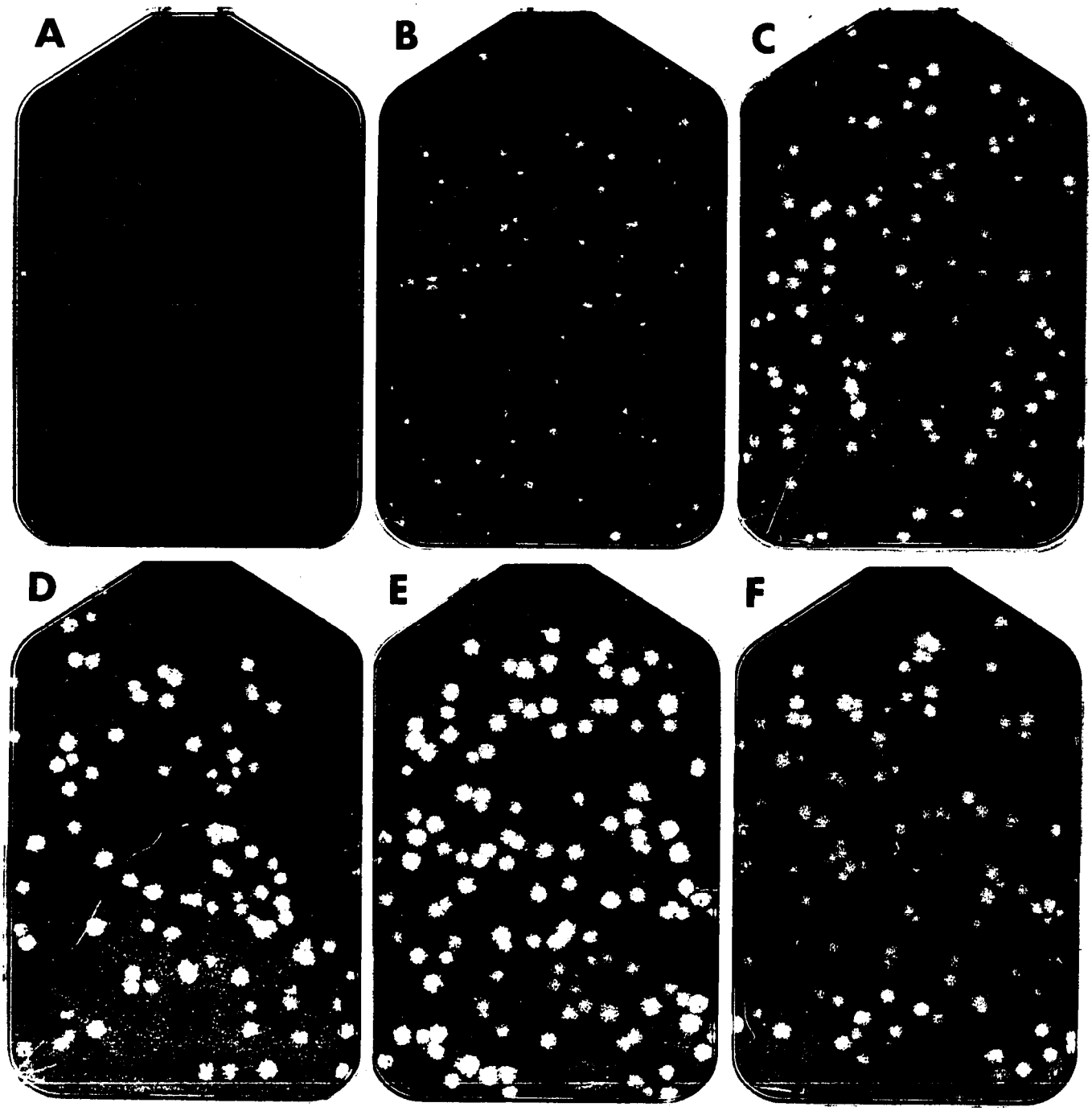
A
B
C
D
E
F

TABLE 2

EFFECT OF MAGNESIUM ON PLAQUE NUMBER AND SIZE

Dilution of Virus Inoculated	Magnesium Chloride	Number of Plaques	Plaque diam., mm
10^{-5}	+	145	4.5
	-	178	4.9
10^{-6}	+	13	3.7
	-	15	4.3

TABLE 3

COMPARISON OF EFFECT ON PLAQUE DEVELOPMENT OF DIFFERENT AGARS IN THE TEST OVERLAY

Trial	Average Number of Plaques per Flask		
	Ionagar #2	Agar #1	Noble Agar
#1	91.8 (6)*	114.5 (2)	87.5 (2)
#2	36.3 (3)	41.7 (3)	N.D.

* Numbers in parentheses indicate the number of flasks in the sample.

N.D. = Not done.

slightly more numerous than those under media with the other agars; plaques under Noble Agar overlays were smallest.

f. Final Medium

On the basis of the above data, several modifications were made to the test overlay: reduction of the BUdR concentration to 50 µg/ml from 100, increasing the DEAE-dextran to 200 µg/ml from 100 and substitution of Agar #1 for Ionagar #2. The final formulation was therefore: Medium 199 containing 0.2% $NaHCO_3$, 50 µg/ml of BUdR, 200 µg/ml of DEAE-dextran, 2% fetal calf serum, 0.6% Oxoid Agar #1 and antibiotics. In this final form, the overlay was used for the titration of virus in all subsequent experiments.

ii) Time Required for Plaque Development

In earlier experiments we had observed that plaques may or may not be detectable on the third day following infection therefore we examined only the period beginning on the fourth day. A pool of diluted virus was prepared and aliquots were inoculated into ten flasks each of W1-38, L 132 and HFL (HF-62-L) cells. Overlay medium was added as previously and cultures were incubated at 33°C. Flasks were removed from the incubator, fixed and stained at the indicated times. Plaques were counted and the diameter of ten randomly selected plaques from each cell line was measured and averaged for each day's sample.

These results are presented in Table 4 and Figures 7 and 8. It was noted that the monolayers appeared healthy and well maintained throughout the period of study (11 days), i.e. there was no cell sloughing or obvious degeneration in any flask.

Plaques were produced in all three cell lines, with four fold higher titres in L 132 cells than in Wl-38, which was in turn more sensitive than HFL. This was in contrast to an earlier result where the titres in L 132 and another HFL line (HF-26-L) were equivalent (see pages 13-14). Several factors may have contributed to this difference: the difference in cell strains, the changes in the overlay and the fact that the virus used in the present study had had seven or eight consecutive passes in L 132 cells while the former inoculum was pooled material from Wl-38 and L 132 grown virus.

No increase in plaque numbers per flask was detected over the period studied (4-11 days post inoculation). The assay in L 132 cells was readable at 4 days but the average plaque diameter was less than two millimeters and many of them measured less than 1 mm; by day 6 the minimum size was about 1 mm while the average was 3.5 mm (Figure 8). Plaques in the latter size range are not likely to be confused with irregularities in the monolayer, so 6 days was chosen as the standard incubation time on this basis although shorter incubations are feasible. Similarly, plaques on both the diploid cell lines were difficult to detect on day 4 while

TABLE 4

NUMBER AND SIZE OF PLAQUES AT DIFFERENT TIMES POST-INFECTION IN THREE CELL LINES

Incubation Time, Days	L 132		Wl-38		HF-62-L	
	Number	Diam, mm.	Number	Diam, mm.	Number	Diam, mm.
4	64	≤2	ca. 13	?	ca. 12	?
5	78 101	2.4	19 13	3	15 11	3
6	67 68	3.5	13 21	4.5	7 13	3.8
7	75 73	4.4	22 25	6.3	17 21	5.7
8	77 88	5.0	22 14	7.9	13 17	7.3
11	69	5.9	15	12	11	10
Averages	76.0		17.7		13.7	

FIGURE 7

Figure 7:- Plaque production in three cell lines after varying periods of incubation. Open circles, L 132 cells; extensions define the confidence limits based on Poisson distribution ($\pm 2\sigma$). X's, Wl-38 cells; triangles, HF-62-L. In all cells, plaque number remained constant throughout the period studied.

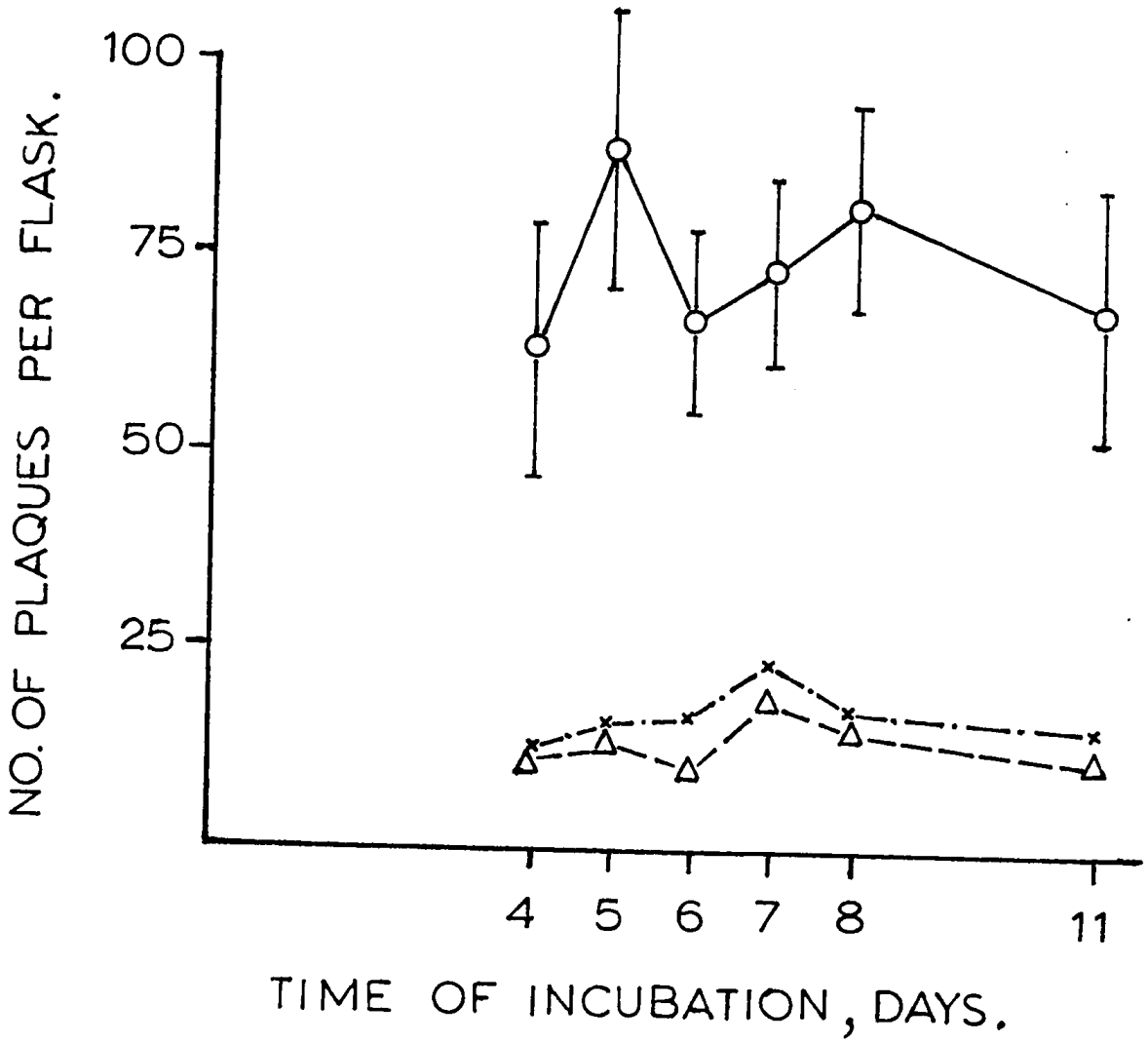
100
75
50
25
NO. OF PLAQUES PER FLASK.
4
5
6
7
8
11
TIME OF INCUBATION, DAYS.

FIGURE 8

Figure 8:- Effect of length of incubation on plaque size. Open circles, L 132 cells; X's, Wl-38; triangles, HF-62-L. Although plaques could be seen and counted in Wl-38 and HF-62-L cells on day 4, they were ill-defined, precluding measurement of diameter.

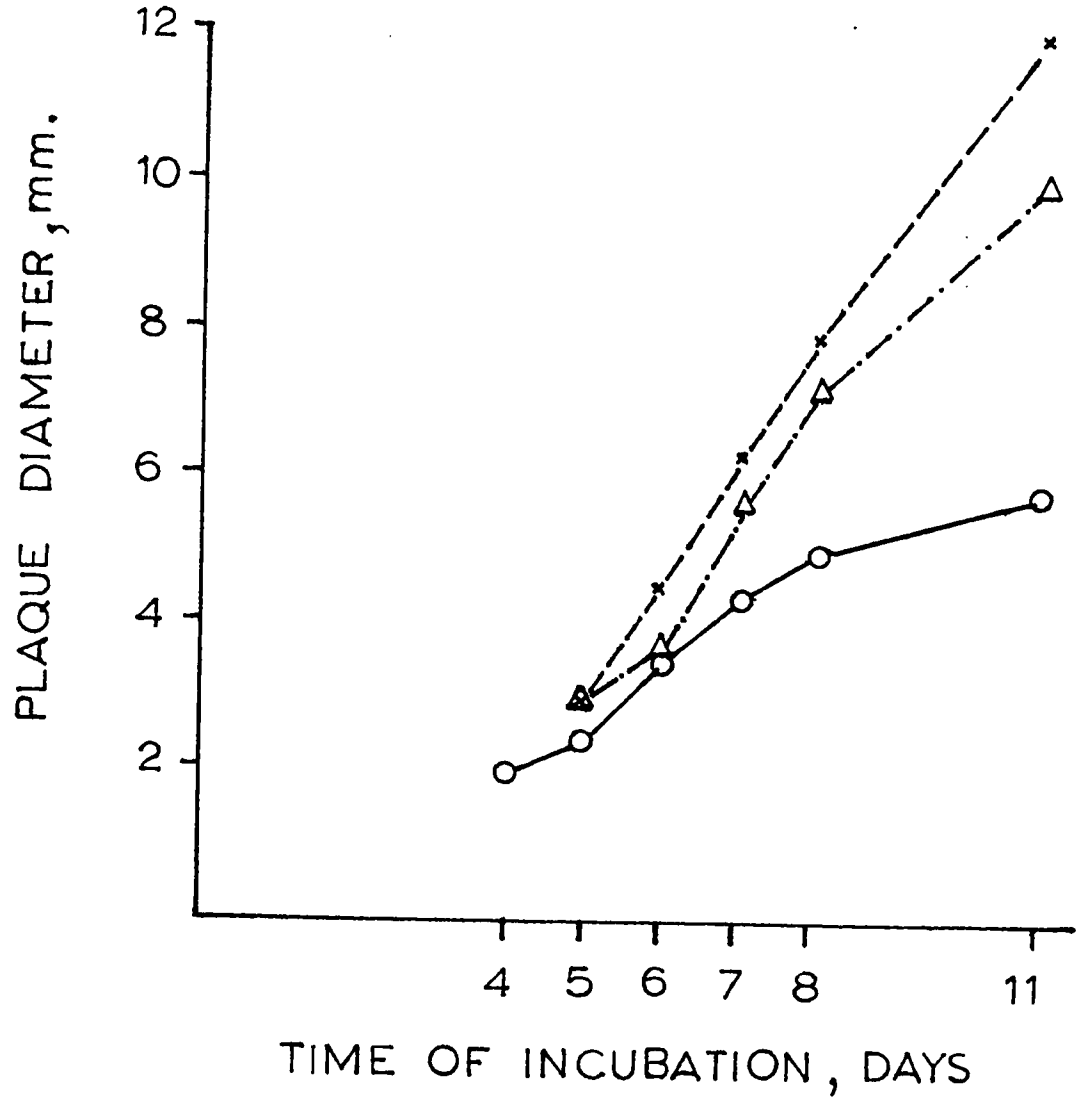
PLAQUE DIAMETER, mm.
12
10
8
6
4
2
4
5
6
7
8
11
TIME OF INCUBATION, DAYS

by day 6 they could be counted with ease.

iii) Dose-Response Curve

Six inocula were prepared from a common pool, each requiring only one further dilution step to give relative virus concentrations in the range of 1 to 10. Aliquots from each of these were assayed in triplicate.

The results of these determinations are presented in Table 5 and Figure 9. The number of resulting plaques varied in direct proportion to the dose of virus applied to the flasks as would be expected on the assumption that a single infectious unit gives rise to a plaque.

A second feature of the data is that good agreement between expected titres and actual counts was maintained up to 300 plaques per flask. This limit is higher than those recommended by several authors (Dulbecco and Vogt, 1954; Cooper, 1961; Lorenz and Zoeth, 1966) who noted that overlapping of plaques led to losses of counts at high levels. However, we have observed that plaques in our system remain discrete even when quite crowded (Figure 10) which probably accounts for the wide range of agreement. The increasing underestimation of titre seen at 400 and 500 plaques per flask is typical of the overlap effect noted by the authors referred to above, but it should be noted that statistical agreement was maintained even at 400 plaques per flask, while the error at 500 per flask was less than 10%. Thus, this plaque assay system produced reasonable

TABLE 5

NUMBER OF PLAQUES PRODUCED AT DIFFERENT VIRUS CONCENTRATIONS

Relative Concentration	No. of Plaques	Mean ($\bar{x}$)	Standard Error ($\sigma=\sqrt{\frac{\bar{x}}{n}}$)*	Confidence Limits ($\bar{x} \pm 2\sigma$)
1	50 31 54	45	3.9	37.2-52.8
2	101 100 115	105.3	5.9	93.5-117.1
4	209 192 230	210.3	8.4	193.6-227.0
6	300 324 294	306	10.1	285.8-326.2
8	425 354 355	378	11.2	355.6-400.4
10	455 451 480	462	12.4	437.2-486.8

* Standard error of the mean, assuming Poisson distribution.

FIGURE 9

Figure 9:- Dose-response curve for plaque production in L 132 cells. Data obtained are represented by open circles and confidence limits for these points are indicated. The solid line represents a linear relationship between plaque numbers and virus dose while the two companion curves represent the result expected if 2 co-infecting particles were required to initiate a plaque (Dulbecco and Vogt, 1954). One curve is extrapolated from the highest (theoretical) plaque number, the other from the lowest. The data obtained are clearly a better fit to the linear relationship.

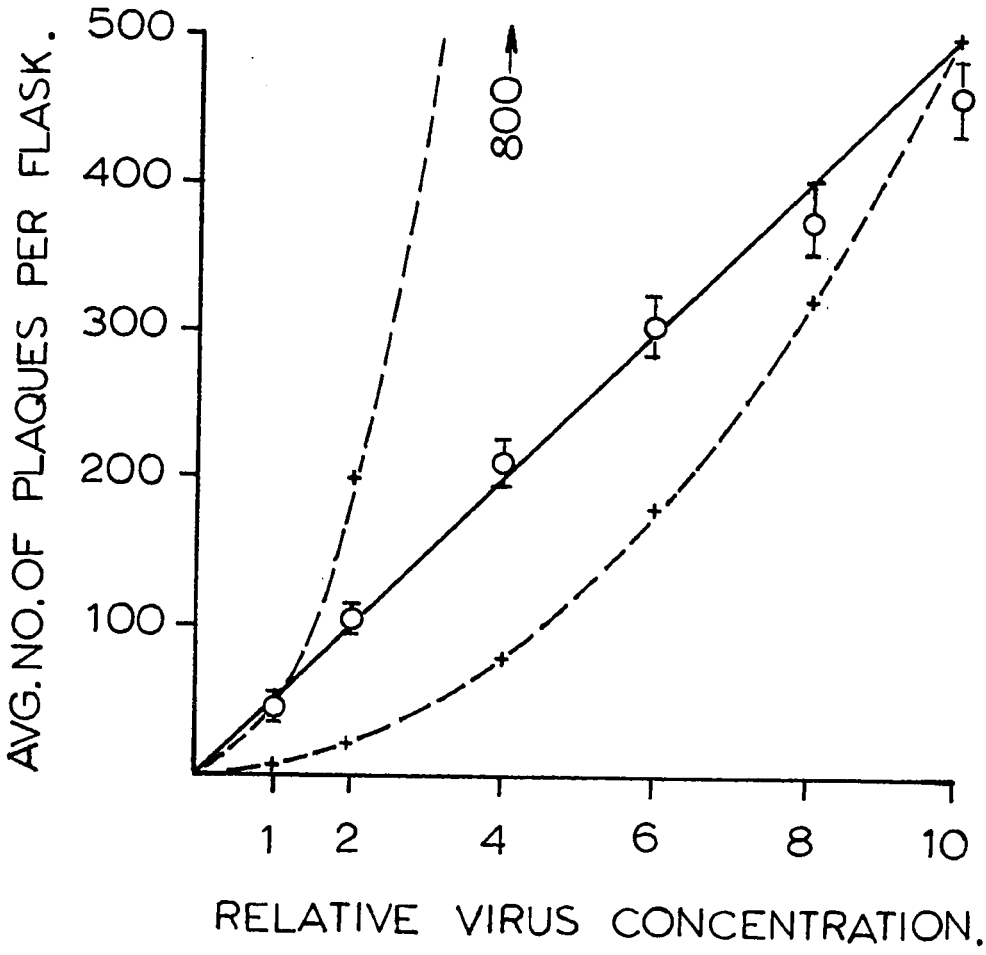
AVG. NO. OF PLAQUES PER FLASK.
500
400
300
200
100
800
1
2
4
6
8
10
RELATIVE VIRUS CONCENTRATION.

FIGURE 10

Figure 10:- Morphology of plaques on a monolayer of L 132 cells infected with 229E after fixation and staining. It can be seen that a ridge of cells (arrows) usually remains between adjacent plaques, even when they are quite crowded, as in this illustration. The edge of a millimeter rule is included at the right hand margin of the photograph.

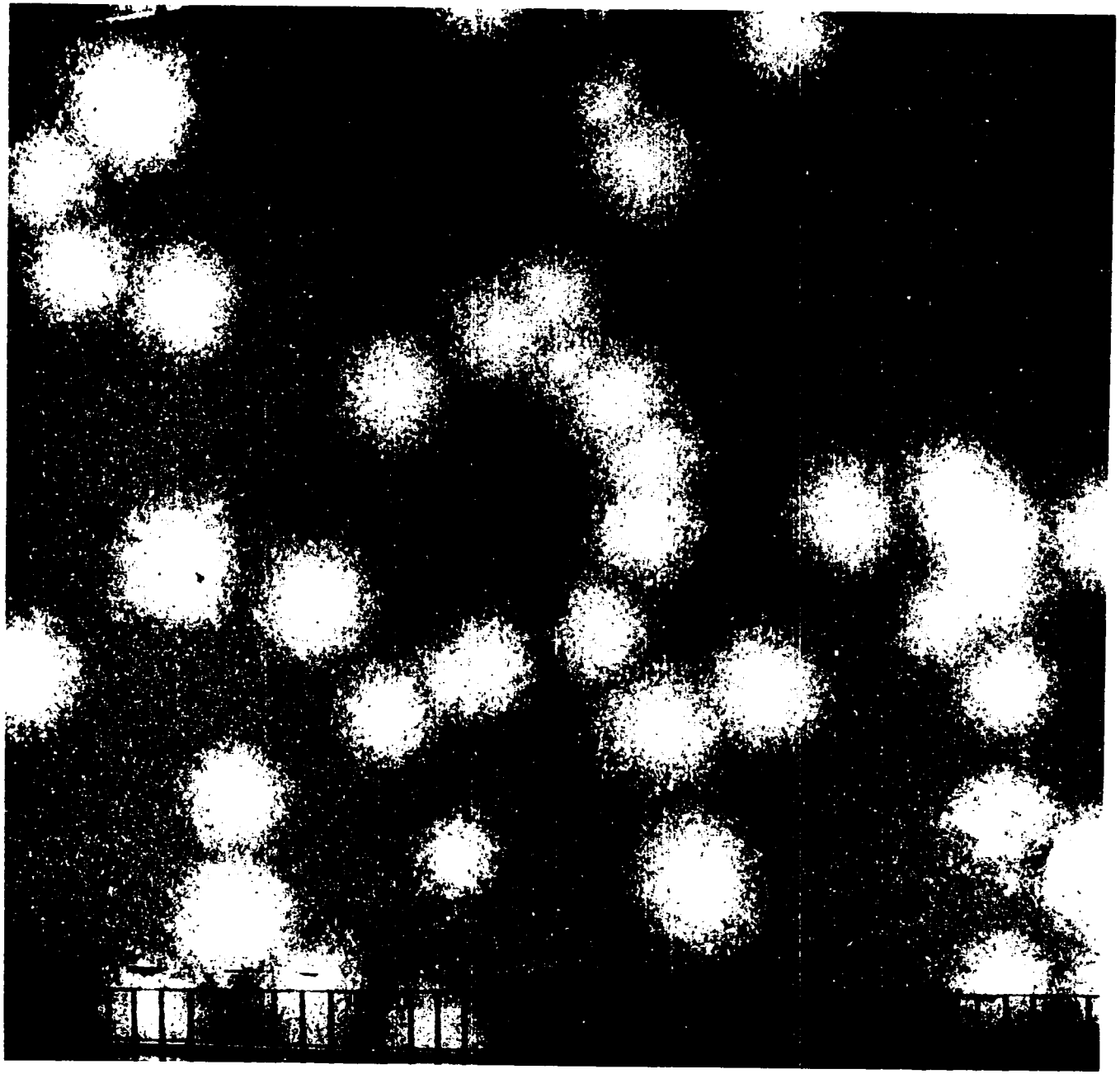

estimates of virus titre over the entire range examined. With small numbers of plaques per flask, the standard errors in individual counts become quite large (e.g. Table 1/8/6 in Reid, 1968) and thus the lower useful limit of the assay will be determined by the statistical limits of reliability required in a given experiment.

iv) Observations Regarding Reproducibility

a. Distribution of Plaque Counts Among Replicate Cultures

Retrospective statistical analysis of plaque assay data by the X^2 test of variance ratios (Snedecor and Cochran, 1967) indicated that individual plaque counts from replicate cultures varied according to the Poisson distribution. Confidence limits based on this distribution are plotted for some of the data presented in Figures 7 and 9 and were calculated according to the formulae presented by Dulbecco (1973).

b. Effect of Re-Using Culture Flasks

In Table 6 there are data from a set of 10 cultures which were inoculated with aliquots from the same virus suspension. Four of these cultures were in bottles which had been used previously for cell growth, trypsinized and reseeded, the other 6 were contained in flasks used for the first time. It was noted that the 2 groups formed 2 barely overlapping distributions, with the average titre in the new flasks being 25% higher than the average in the

TABLE 6

EFFECT OF RE-USING FLASKS ON PLAQUE NUMBERS

	Number of Plaques per Flask	
	New Flasks	Re-Used Flasks
	124	112
	138	102
	126	101
	135	88
	110	
	120	
Averages	125.5	100.8

re-used flasks.

These data provided confirmation of many individual observations in which it was noted that disagreement between replicate assays followed the same pattern, i.e. consistently more and sometimes larger plaques were formed in new flasks than were formed in "old" ones. The cause of this depression in plaque counts is not known, but since we have observed that cell cultures reached confluence significantly more quickly in re-used flasks, perhaps this result is indicative of a decline in sensitivity of L 132 cells with increasing age as a monolayer. Such an effect has been noted by Valle (1971) regarding the sensitivity of chick embryo fibroblast cultures to vesicular stomatitis virus.

c. Effect of Passage Level of L 132 Cells Used in the Assay

The passage level of these cells on reaching this laboratory was unknown, but since then they have undergone up to 75 population doublings. A review of our data revealed that on several separate occasions we have assayed aliquots of the same virus in both high passage and low passage level cells. The results indicate that high passage cells are less sensitive to virus than are low passage, at least as expressed by plaque production (Table 7). In experiments 1 and 2 in Table 7 the high and low pass cells were inoculated from the same diluted suspension in the course of a titration whereas in example 3, two separate titrations of the same stock are given. The result is that

TABLE 7

VARIATION IN VIRUS TITRE USING CELLS AT DIFFERENT PASSAGE LEVELS

Experiment Number	Low Passage		High Passage		Ratio
	Pass Level*	Titre	Pass Level	Titre	Low/High
1	15	3.1×10^8	52	1.6×10^8	1.9
2	14	2.2×10^6	35	1.2×10^6	1.8
3**	20-25	5.1×10^7	47	1.7×10^7	3.0

* Refers to level in this laboratory, absolute value unknown.

** Aliquots of the same frozen stock, but on 2 separate occasions.

consistently higher titres were obtained when low passage cells were used for plaque assays.

Corroborating data was provided by an experiment in which cultures were inoculated for virus growth. Two different inocula were used, and each was used to infect 3 monolayers of cells at passage 14 and 3 at passage 35. Cultures were infected at low input multiplicity (IM) and incubated 40 hours at 33°C. When pooled batches were titrated, the ratio of yield from pass 14 cells/yield from pass 35 cells was 1.9 and 2.7 in the two trials. These ratios are similar to those obtained from the plaque assay trials, and together, both lines of evidence suggest that L 132 cells may become less sensitive to 229E with continued passage in the laboratory. Indications of a similar change in sensitivity have been noted for the SV_{40}/BS-C-1 system (Hopps et al., 1963).

These findings were not investigated further but are recorded here as they reflect on circumstances which affect the plaque assay.

v) Applicability to Other Viruses

The plaque assay essentially as described above was used for the titration of both poliovirus (Sabin Type I) and vesicular stomatitis virus (Indiana serotype). VSV required 3 days for good plaque development at 33°C (negligible proportion of plaques less than 1 mm diameter) whereas poliovirus plaque development was complete in 2 days

at 37°C by the same criterion. The addition of 30 mM $MgCl_2$ led to the production of larger, more uniform plaques with poliovirus (Wallis and Melnick, 1962). Although comparisons between this medium and others used for these viruses were not done, titrations of yields of VSV and poliovirus obtained from L 132 cells gave values of 2100 and 1200 pfu/cell respectively, indicating that the assay was adequately sensitive.

Discussion and Conclusions

We have developed an overlay based on Medium 199 for the production of plaques by coronavirus 229E in monolayer cultures of L 132 cells. The overlay is used in sealed flasks which are incubated in normal atmospheres and it allowed plaque production under these conditions, a result which we were not able to duplicate using other published formulations.

Plaque development is essentially complete after 4 days of incubation at 33°C although increasing the time to 6 days permits development of larger lesions which can be enumerated with greater certainty. The number of plaques produced under this overlay is proportional to virus dose when up to 400 are counted per 75 cm^2 flask and the variation encountered in replicate assays may be accounted for on the basis of random sampling errors, provided that specified conditions are followed in the preparation of cultures.

The medium can be used for the assay of 229E in two lines of diploid fibroblasts (Wl-38 and HFL) in addition to L 132 cells although titres obtained may be lower in the former cells. Furthermore the medium was suitable for plaquing vesicular stomatitis virus and poliovirus, the latter application being aided by supplementation of the medium with $MgCl_2$.

II. EFFECT OF ACTINOMYCIN D ON THE REPLICATION OF 229E

Introduction

The decision to examine the affect of Actinomycin D (AMD) on the replication of coronavirus 229E was made for several reasons, not the least of which was the finding by Tannock (1973) of an apparently heterogeneous nucleic acid in avian infectious bronchitis virus (IBV). Although this finding may have been an artifact generated by the method used for RNA extraction (Watkins et al., 1975), at the time, it provided the incentive which led us to explore the interaction between 229E and Actinomycin D. As it had been shown that viruses from other taxonomic groups may include non-viral nucleic acid in the virion, (Michel et al., 1967; Siegel, 1971; Pedersen, 1971) we postulated that coronaviridae may have this tendency in large degree, contributing to the situation found by Tannock. We therefore proposed to label viral nucleic acid under conditions where host RNA synthesis was repressed, extract virion nucleic acid and compare our results to those of Tannock. AMD was chosen to repress cellular RNA synthesis because its function in that role has been well documented (Reich et al., 1962; Reich and Goldberg, 1964; Meienhofer and Atherton, 1973).

In addition to the above rather speculative proposal, an examination of the effect of AMD on 229E would be of general benefit: if 229E was refractory to the effects of this drug, then AMD could be used to selectively inhibit host transcription, facilitating the study of viral replicative functions. If, on the other hand, the virus was inhibited by AMD, this fact in itself would provide insight into the viral mode of replication.

In fact, the effect of AMD on the replication of several members of the coronavirus group has been examined by other workers. Parker et al. (1970) reported that 1 µg/ml of AMD had no effect on the replication of rat coronavirus (RCV) as measured by induction of CPE or development of viral antigens detectable by fluorescent antibody, but gave no details of the pertinent experiments. Malluci (1965) grew mouse hepatitis virus (MHV) to normal titres in mouse macrophage cultures in the presence of 0.01 and 0.05 µg/ml of this drug, and Bingham (personal communication, C. M. Johnson-Lussenburg) found avian infectious bronchitis virus (IBV) insensitive to AMD. On the other hand, Clarke (1968) grew transmissible gastroenteritis virus of swine (TGE) in the presence of 0.2 µg/ml, and observed 84 to 92% reduction in yield of virus at 18 hours post-infection, depending on the mode of exposure to AMD; and Lomniczi (1975) also reports "0.2 µg" reduced the yield of IBV to 3% of control values when tested in chicken lung cultures, whereas 10-fold greater concentrations were needed to produce the same degree of inhibition when kidney

cultures were used for virus growth.

In our studies on the human coronavirus strain 229E, because the effects of AMD on cellular metabolism are known to vary with cell type (Sawicki and Godman, 1973; Biedler and Riehm, 1970) and with concentration (Perry, 1963), it was decided to include controls which would give some indication of the state of the AMD treated cells. Vesicular stomatitis virus (VSV) has been shown to replicate independently of host cell nuclear function in that it is not affected by AMD (Black and Brown, 1968; Yamazaki and Notkins, 1973) and in fact it multiplies to normal levels in enucleated cells (Follet et al., 1974; Wiktor and Koprowski, 1974). Thus, if it could replicate normally at the concentrations of AMD used in our experiments, this would indicate that the cells had maintained a level of integrity appropriate to the replication of at least one RNA virus. In contrast to VSV, adenovirus is inhibited by AMD (e.g. Wigand and Schmeider, 1973) and was included as an AMD sensitive virus. The incorporation of tritiated uridine into acid-precipitable material was followed as an indicator of the effect of AMD on the host cell's RNA metabolism. Thus, these controls would provide a framework to aid in the evaluation of any effects of AMD on 229E.

Materials and Methods

i) Preparation of Tube Cultures

Tube cultures of L 132 cells were prepared in 16 x 150 mm glass test tubes. Cultures were seeded with

approximately 3 x 10^5 cells per tube in 1.5 ml of growth medium (MEM with 10% FCS and antibiotics), stoppered, and incubated at 37°C for 2-3 days until formation of a monolayer. Immediately before infection, 3 tubes were selected at random, trypsinized and the cells counted in a haemacytometer.

ii) Actinomycin D Stocks

Actinomycin D (Dactinomycin; Merck, Sharp and Dohme) was prepared as a stock solution at a level of 1000 µg/ml in sterile distilled water, dispensed in 200 or 500 µl amounts and stored frozen at -70°C until required.

iii) Dose-Response Curves

a. 229E

Dilutions of virus were prepared to achieve an input of 3 pfu/cell in 0.1 ml volume (actual range = 2.5 to 5 pfu/cell). Tube cultures, prepared as described in i), above, were drained of growth medium, 0.1 ml of virus suspension per tube was added to each and the cultures were held at room temperature for an adsorption period of 1 hour. During the adsorption period, virus was redistributed over the monolayer at 15 minute intervals. At the end of this period, 1.5 ml of medium 199 containing 0.2% BSA and the appropriate amount of Actinomycin D was added to each culture and the tubes were incubated at 33°C for 40-42 hours. Triplicate cultures were used for each level of AMD.

After incubation the cultures were subjected to 2 freeze-thaw cycles, replicate cultures were pooled, and

dispensed into vials which were refrozen to await subsequent titration. Titration was by plaque assay as described previously.

b. Vesicular Stomatitis Virus

Permission to use VSV was obtained from the Health of Animals Branch of Agriculture Canada, in accordance with their policies on the use of this agent in Canadian laboratories. The virus itself was obtained from Dr. E. Rossier, University of Ottawa and was of the Indiana serotype (Rossier and Landry-Pigeon, 1972). Obtained as a whole culture lysate of infected Wl-38 cells, it was passaged four times at low multiplicity in L 132 cells before use in the AMD experiment, the second pass being a single plaque isolation.

Cell monolayers were drained and infected with an input multiplicity of 10 pfu/cell. Adsorption of virus and the addition of media were as above. Cultures were incubated at 33°C until 90-100% of the cells had detached from the flask.

After incubation, replicate cultures were pooled and aliquots were dispensed in vials which were then stored at -70°C.

Titrations were done by plaque assay as described for 229E with two exceptions: dilutions were made in BSA Medium (Valle, 1971), and incubation for plaque development was only continued for 3 days, at which time the proportion of microplaques (i.e. < 1 mm diam.) was minimal.

c. Adenovirus

A strain of Adenovirus type 7 was obtained from Mr. P. Phipps (Virus Laboratory, Children's Hospital of Eastern Ontario) as a frozen culture of infected Wl-38 cells. This virus was passed at least 3 times in L 132 cells before use in these experiments.

Tube cultures of L 132 cells were drained and inoculated with 0.1 ml of virus at an input of 7.5 TCD_{50}/ cell. Virus was allowed to adsorb at 37°C for 2 hours, redistributing the inoculum at 30 minute intervals. After adsorption, the cultures were rinsed twice with 1 ml each of PBS/BSA, then incubated with 1.5 ml per tube of M 199/BSA with or without AMD at 37°C for 32 hours.

Following incubation, cultures were freeze-thawed to aid virus release, replicates were pooled, aliquots dispensed and frozen at -70°C until titrated.

Adenovirus was titrated in tube cultures of L 132 cells. Ten-fold dilutions of virus were prepared in M 199/BSA and inoculated at 0.1 ml per tube to each of four tubes per dilution. Cultures were incubated at 37°C for 2 hours for virus adsorption, then a maintenance medium of M 199 with 2% FCS was added, 1.5 ml per tube. Inoculated tubes were incubated at 37°C. The maintenance medium was replaced at three or four day intervals and the tubes were examined and scored for CPE on the day following a medium change. Titres were calculated according to the method of Reed and Muench as described by Lennette (1969) and

converted to TCD_{50} per ml.

d. RNA Synthesis

The growth medium was removed from confluent tube cultures of L 132 cells, replaced with M 199/BSA with or without appropriate levels of AMD and the tubes were placed in a 33°C incubator for a preincubation period of 1½ hours. Duplicate cultures were used for each test condition.

Following preincubation, 100 µl of M 199/BSA containing 1.5 µCi of [5-^{3}H]-uridine (sp. act. 29.65 Ci/mmole, New England Nuclear) was added to each tube where appropriate, after which the cultures were incubated at 33°C for 1 hour. Controls included cultures which were held at 0°C throughout the incubation period as well as mock-labelled cultures which had received only an additional 100 µl of maintenance medium prior to incubation.

After incubation, all cultures were removed to an ice bath, the incubation medium was removed and the monolayers were washed twice with 1-2 ml aliquots of PBS (phosphate buffered saline, Ca^{++}, Mg^{++} free). After the second wash, 1.5 ml per tube of PBS was added and the cells were disrupted by 3 freeze-thaw cycles. 1.5 ml of 10% trichloroacetic acid (TCA; Fisher Certified, A.C.S.) was then added to each tube, the contents were mixed and the cultures held at 0°C for 60 minutes to allow precipitation.

The precipitates were then transferred to centrifuge tubes and sedimented at 2000 rpm at 4°C for 10 minutes in an

IEC PR6 centrifuge (1000 x g). Supernatants were discarded and the precipitates washed twice by alternate resuspension in 1.5 ml/tube of 5% TCA and centrifugation. Finally, the precipitates were solubilized in 1 ml/tube of NCS (Amersham/ Searle Corp.) at 48-50°C for 1 hour, after which the digest was neutralized by the addition of 0.03 ml/tube of glacial acetic acid. Neutralized digests were mixed with 10 ml per sample of scintillation cocktail (6 g/l of PPO in toluene) and transferred to polyethylene vials for counting in a Beckman LS-250 scintillation counter.

iv) Determination of the Growth Curve of 229E

Growth medium was removed from cultures to be infected and 0.1 ml per tube of virus in M 199/0.2% BSA was added to each, at an input multiplicity of 10-20 pfu per cell. Inoculum was distributed over the cell sheet immediately and at 15 minute intervals during the subsequent adsorption period of 1 hour at room temperature.

At the end of the adsorption period, the inoculum was removed from the tubes and the cultures were given two washes of 1.5 ml each of phosphate buffered saline (PBS). After the second wash, 1.5 ml of M 199 containing 0.2% BSA and antibiotics was added to each tube and the cultures were incubated at 33°C. Unincubated (i.e. 0 hour) samples were collected at this time.

At each indicated sampling time, 3 tubes were selected at random, labelled as to length of incubation and

transferred to a -20°C freezer. When the entire schedule had been completed, the cultures were subjected to a thaw-freeze cycle in the tubes, after which replicates were pooled and aliquots dispensed and frozen to await titration. Two separate titrations were done on the samples from each experiment and the titrations were completed within three weeks.

v) Effect of Addition of Actinomycin D At Different Times During the Growth Cycle

Tube cultures were prepared, counted and infected as described for the growth curve experiments, using virus input levels of 11-15 pfu per cell. M 199/BSA was used as maintenance medium and cultures were incubated at 33°C. At intervals post infection, triplicate cultures were removed from the incubator and 100 µl of diluted AMD stock was added to each, giving a final concentration of 2 µg/ml in the maintenance medium. Cultures were then returned to 33°C and incubation continued. At 24-28 hours post infection, all tubes were removed from the incubator and frozen. Subsequent treatment and titration was as described for the growth curve studies.

vi) Effect of Input Multiplicity on Virus Yields

Tubes were prepared for inoculation as described previously. Sets of six tubes were infected using different dilutions of virus, 0.1 ml per tube. Virus concentrations

were such that input multiplicities of 0.8, 3.3, 12.5 and 42 pfu/cell were delivered to 4 sets of 6. After adsorption as before, half of each set received M 199/BSA alone, the other 3 tubes received M 199/BSA containing 1 µg per ml of AMD. Incubation was at 33°C for 28 hours.

After incubation, the cultures were gassed with 5% CO_2 in air before freeze-thawing in an attempt to stabilize the pH during this process. Otherwise the cultures were treated in the same manner post incubation as described previously for tube culture experiments.

Results

i) Dose Response Curves

Yields of 229E from cells incubated in the presence of various levels of AMD were depressed in comparison to yields obtained from parallel cultures not exposed to this drug. The effect was reproducible and the inhibition was proportional to the amount of Actinomycin present during growth (Table 8). When plotted on a semi-logarithmic scale (Figure 11), a direct relation was obtained between yields of 229E expressed as a percentage of control values and the logarithm of the AMD concentration. From this plot the 50% inhibitory dose of AMD under these conditions was estimated to be 0.09 to 0.10 µg per ml. The same data are plotted on linear axes in Figure 12.

When infected and control cultures were examined microscopically, AMD was seen to contribute to cell

TABLE 8

EFFECT OF ACTINOMYCIN D ON THE REPLICATION OF VIRUS

Virus	Input Multiplicity	Concentration of Actinomycin D, micrograms per millilitre						
		0.0	0.01	0.03	0.10	0.32	1.0	10.0
229E	2.5	50* (100%)**	ND	42 (84%)	14 (28%)	14 (28%)	1.8 (3.6%)	<0.3 (<0.6%)
229E	5	110 (100%)	ND	69 (66%)	70 (67%)	29 (28%)	4.5 (4.3%)	ND
229E	4	70 (100%)	65 (93%)	43 (61%)	35 (51%)	9.9 (16%)	1.2 (1.7%)	ND
VSV	10	400 (100%)	440 (110%)	ND	450 (112%)	ND	360 (90%)	250 (63%)
Adeno	7.5	32 (100%)	1.0 (3.1%)	ND	0.3 (1%)	ND	0.3 (1%)	ND

* Virus titres, expressed as pfu/ml x 10^{-6} (229E and VSV) or TCD 50/ml x 10^{-6} (Adeno).

** Numbers in parentheses are percentage yields with respect to Actinomycin-free controls.

ND = Not done.

FIGURE 11

Figure 11:- Effect of Actinomycin D on virus replication and RNA synthesis in L 132 cells. When the concentration of AMD is plotted on a logarithmic axis, as in this example, a linear dose-response curve is obtained for 229E.

EFFECT OF ACTINOMYCIN D ON VIRUS AND RNA SYNTHESIS.

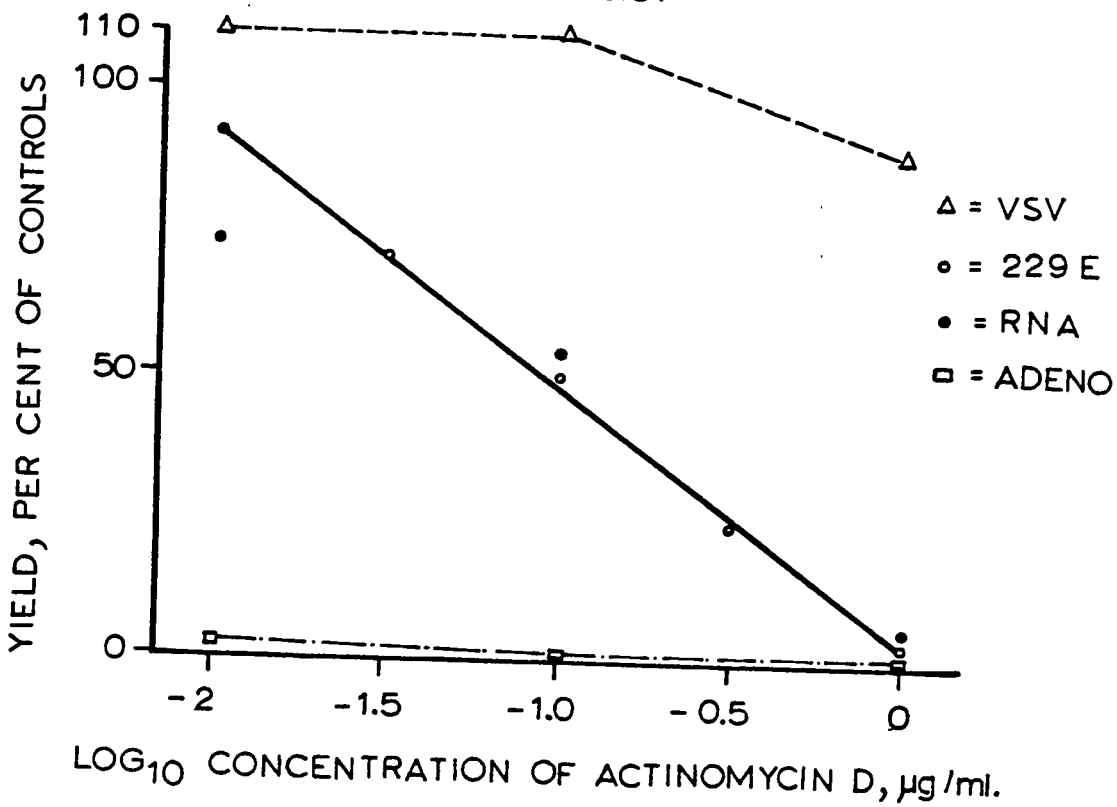

FIGURE 12

Figure 12:- Effect of Actinomycin D on virus replication and RNA synthesis in L 132 cells. Same data as presented in Figure 11, but plotted on linear axes.

EFFECT OF ACTINOMYCIN D ON VIRUS AND RNA SYNTHESIS.

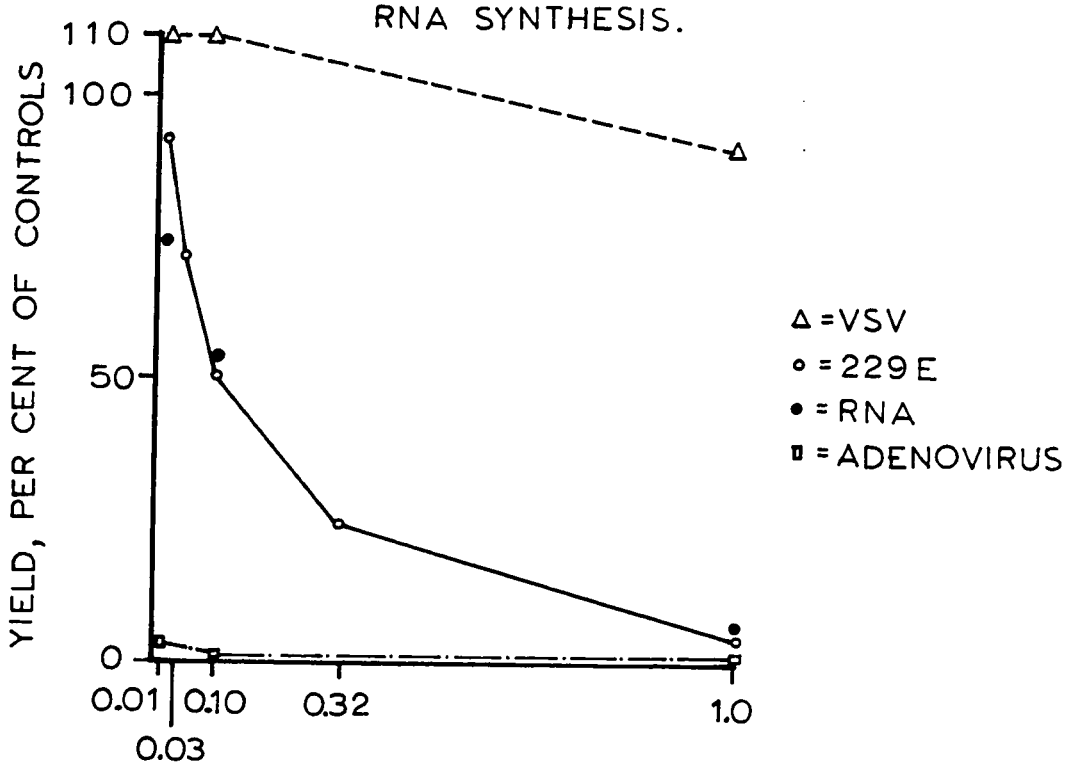

rounding, possibly implying a toxic effect; for example, at 40 hours post infection, cultures containing 0.1 µg per ml or higher had more rounded cells than AMD-free controls, while cultures containing 1 or 2 µg per ml were detectably different from controls at 16 to 19 hours post infection.

Companion experiments examined the yields of vesicular stomatitis virus and adenovirus in the presence of AMD. From the data in Table 8, it can be seen that VSV, another large RNA virus, was able to replicate normally in the presence of up to 1 µg per ml of this antimetabolite, ten times the 50% inhibitory dose for 229E, while 10 µg per ml still permitted virus replication to 63% of control levels. In contrast, adenovirus, a double-stranded-DNA virus, was markedly inhibited by even the lowest concentration tested. Ninety-seven percent inhibition of virus production was obtained at 0.01 µg per ml, while at 0.1 µg and greater only 1% of control levels were reached. The persistence of a 1% yield at 10-fold and 100-fold higher concentrations of AMD is somewhat problematical, but may represent a stable residuum of the inoculum.

The incorporation of ^{3}H-Uridine into acid precipitable radioactivity also declined in AMD treated cultures with respect to controls (Table 9) and the dose-response curve appears to coincide with that of 229E. This coincidence is fortuitous in the sense that data from another series of experiments indicates that AMD-induced inhibition of uridine incorporation is progressive over a period of

TABLE 9

EFFECT OF ACTINOMYCIN D ON RNA SYNTHESIS IN L 132 CELLS

	$0^{o}C$ Control	Concentration of Actinomycin D, µg/ml				
		0.0	0.01	0.1	1.0	10
Sample 1	0.30*	147.4	94.6	87.3	10.1	1.04
Sample 2	0.22	142.0	119.7	68.2	8.6	1.02
Average	0.26	144.7	107.1	77.8	9.3	1.03
Average-0^{o}	0.00	144.4	106.9	77.5	9.1	0.77
% of AMD-free Controls	0.2	100	74	54	6.3	0.5

* CPM x 10^{-3} present in acid precipitate of cell cultures after labelling with ^{3}H-uridine.

several hours, extending beyond the pulse period employed in this experiment (data not shown). In analyzing the data obtained in the experiment shown, it was noted that there was very little incorporation at ice bath temperatures and the counts obtained were assumed to be due to non-specific adsorption or entrapment of label; therefore incorporation was calculated by subtracting the 0^{o} values from those obtained at 33^{o} to correct for background and non-specific radioactivity.

ii) Growth Curve of 229E

Since we had found the replication of 229E virus to be sensitive to Actinomycin D, we next examined the time course of inhibition in relation to the virus growth cycle. A growth curve was obtained by infecting L 132 cells in tube cultures, removing cultures at various times post infection and assaying them for virus content after freeze-thawing to aid in virus release. No attempt was made to distinguish between cell-bound and released virus.

Data were obtained from experiments conducted on two sampling schedules. Results are presented in Figures 13 and 14. Summarizing, recoverable virus declined between 0 and 6 hours post infection, then began to increase between hour 6 and hour 9, continuing to a maximum titre at around 24 hours after inoculation. Cultures incubated longer than 24 hours show a progressive loss in titre with the curve falling to about 60% of peak height by 48 hours.

FIGURE 13

Figure 13:- Growth curve of HCV/229E in L 132 cells. Data are from a single experiment, plotted on semi-logarithmic axes.

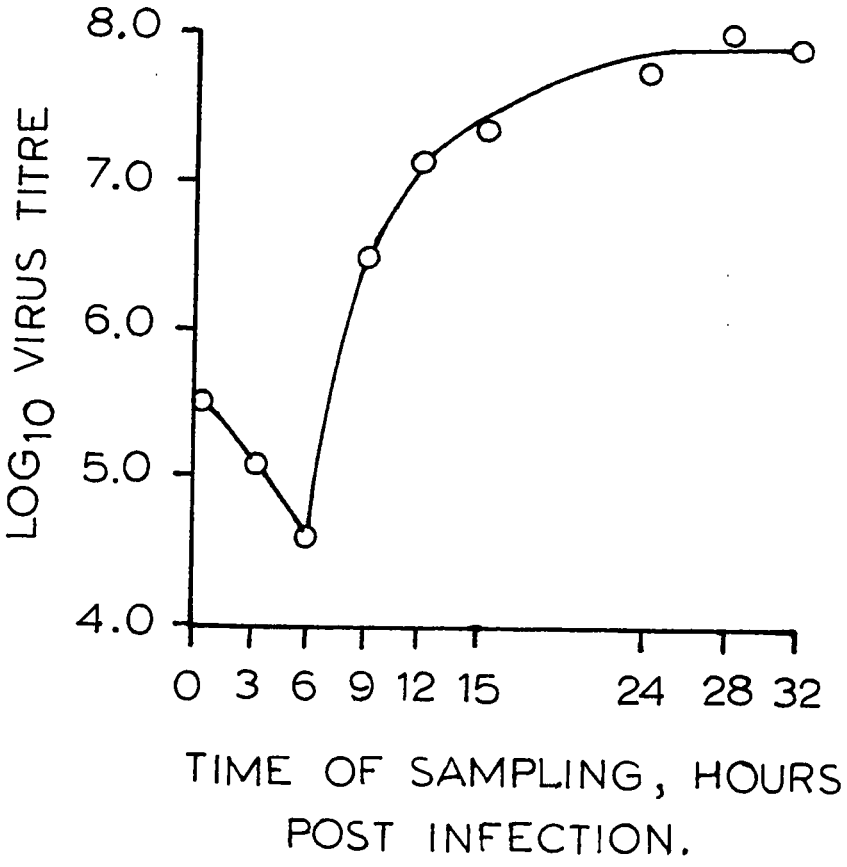
8.0
7.0
6.0
5.0
4.0
LOG10 VIRUS TITRE
0 3 6 9 12 15 24 28 32
TIME OF SAMPLING, HOURS POST INFECTION.

FIGURE 14

Figure 14:- Growth curve of HCV/229E in L 132 cells. Data points plotted are averages from two or three separate experiments.

GROWTH CURVE: CORONAVIRUS 229E IN L132 CELLS

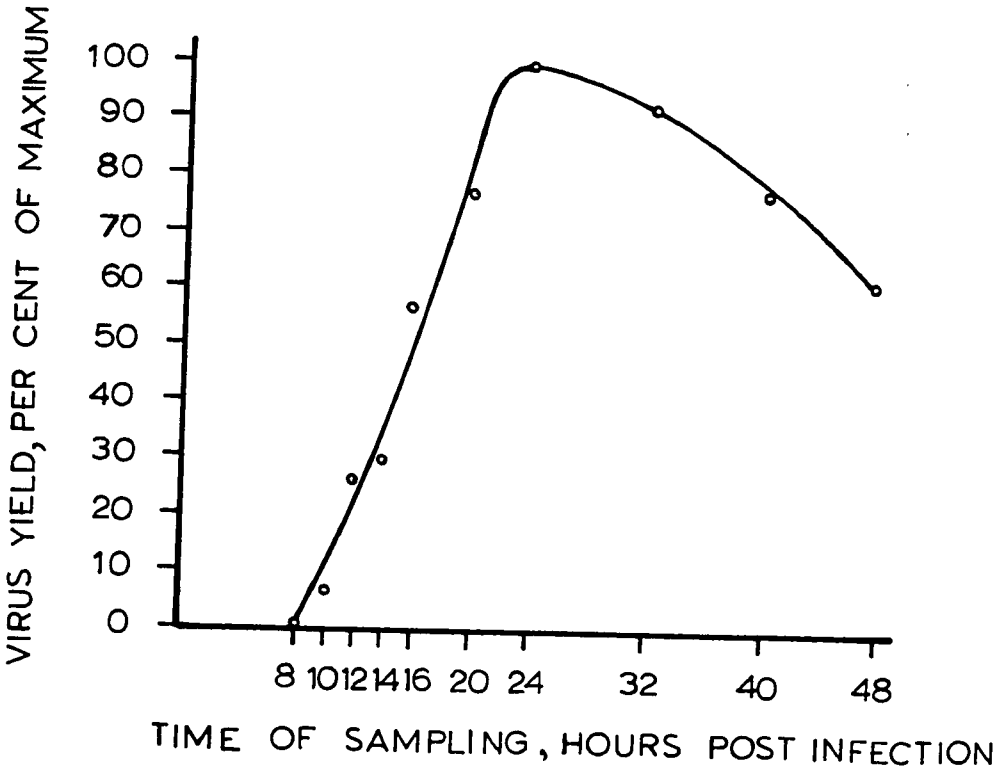

iii) Effect of Addition of Actinomycin D at Different Times During the Virus Growth Cycle

Having obtained evidence that the production of 229E in L 132 cells was inhibited by AMD and having determined the growth curve for the virus in the same cell line, we next examined the effect of adding the drug at various times post infection to see if we could delineate the sensitive step in time.

Inhibition of 229E was maximal when AMD was present throughout the growth cycle, being proportionately less when the drug was added later in the course of replication. Data from individual experiments were converted to a common base as percentage inhibition of treated cultures with respect to drug-free controls and are presented in graphical form in Figure 15. These curves indicate an initially high level of inhibition when Actinomycin is added early in the growth cycle. Later additions, up to a point 8 or 10 hours post-infection show a slight and progressive decrease in the inhibition obtained; at about 8-10 hours however, the inhibition curves change slope and the effect of the drug rapidly diminishes, appearing to have no further deleterious effect after 16 hours. There are some minor inconsistencies in the data presented, but the features described are common to all 3 experiments, seeming to imply that the target reaction for AMD inhibition is maximally sensitive in the first 10 hours of the replicative cycle and non-functional or at least non-essential after 16 hours post-infection.

FIGURE 15

Figure 15:- Inhibition of replication of 229E by Actinomycin D (2 µg/ml) added at indicated times post-infection. Results from three experiments, indicated by closed circles, open circles and triangles respectively.

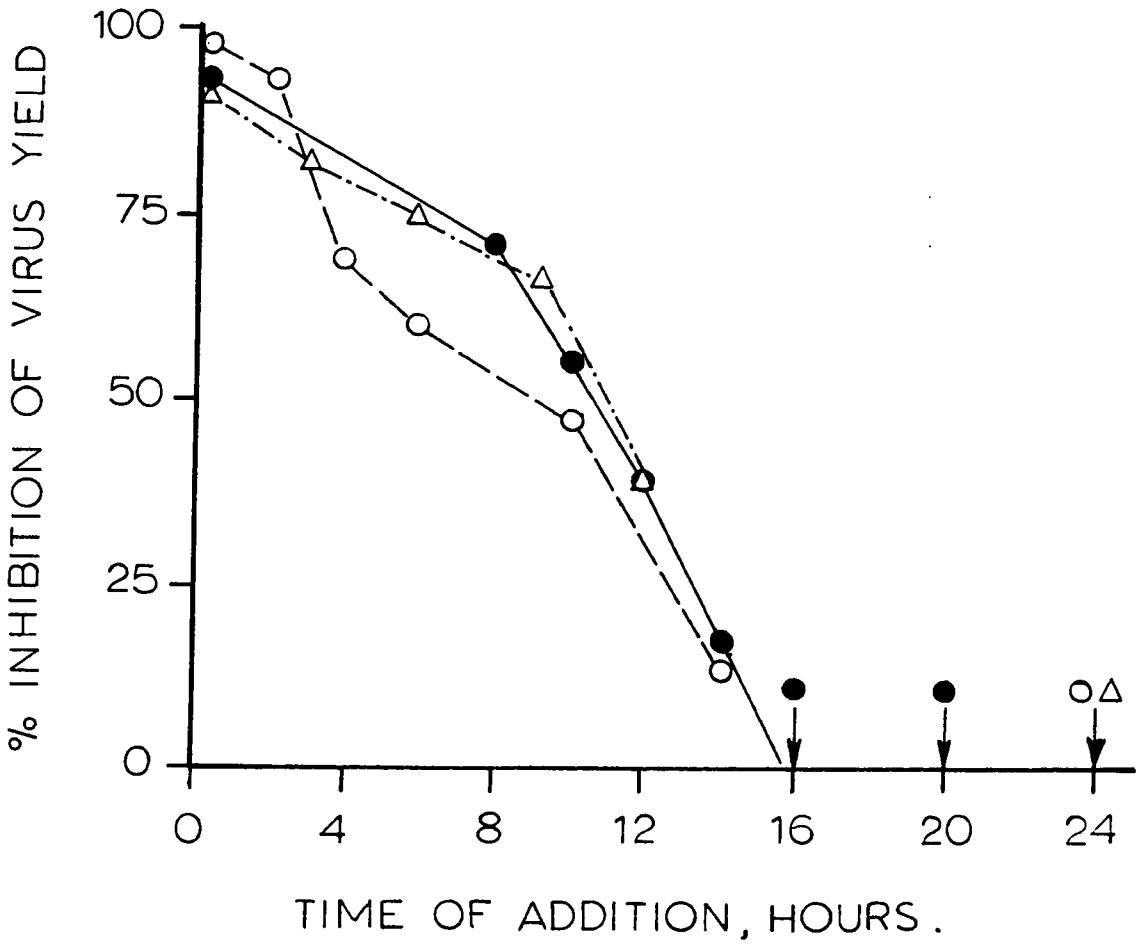
% INHIBITION OF VIRUS YIELD
100
75
50
25
0
0
4
8
12
16
20
24
TIME OF ADDITION, HOURS.

iv) Effect of Input Multiplicity on Virus Yields

Several experiments, both with 229E and with a Sabin strain of poliovirus (data not shown) had suggested that the degree of inhibition produced by a given dosage of AMD might vary with the multiplicity of virus used to initiate the infection. Accordingly, an experiment was set up comparing yields of 229E from cultures infected at four different input multiplicities in the presence and absence of a single level of AMD (1 µg/ml).

Two trends were evident in the data obtained from this experiment (Table 10, Figure 16): in the first place the yield of virus obtained from AMD treated cultures does increase with increasing virus input; and secondly, the opposite effect was seen in the untreated cultures, in that decreased yields were obtained from cultures receiving the higher virus concentrations. Combining these two curves magnifies the apparent effect and the difference between the cultures receiving an IM of 0.8 and those receiving 42 pfu/cell is almost twenty-fold when expressed as percentage yields (Table 10). Whatever the reason for these trends, and several possibilities will be discussed later, it is evident that the virus multiplicity used to initiate the infection will indeed affect the magnitude of the response to AMD.

TABLE 10

EFFECT OF INPUT MULTIPLICITY ON VIRUS YIELD

Input Multiplicity (pfu/cell)	Control (No AMD)	AMD, 1 µg/ml	
	Titre (pfu/mlx10^{-6})	Titre (pfu/mlx10^{-6})	% Yield
0.8	99.5	1.3	1.3
3.3	80.5	2.2	2.7
12.5	59.5	6.9	11.6
42	40.0	7.6	19.0

FIGURE 16

Figure 16:- Effect of input multiplicity on virus yield at 28 hours post-infection in the presence and absence of Actinomycin D. When 1 µg/ml of AMD was present throughout the incubation period, higher yields were obtained with greater virus input (triangles). The opposite effect was seen in untreated cultures (open circles). Arrows indicate the multiplicities used in this experiment: 0.8, 3.3, 12 and 42 pfu/cell.

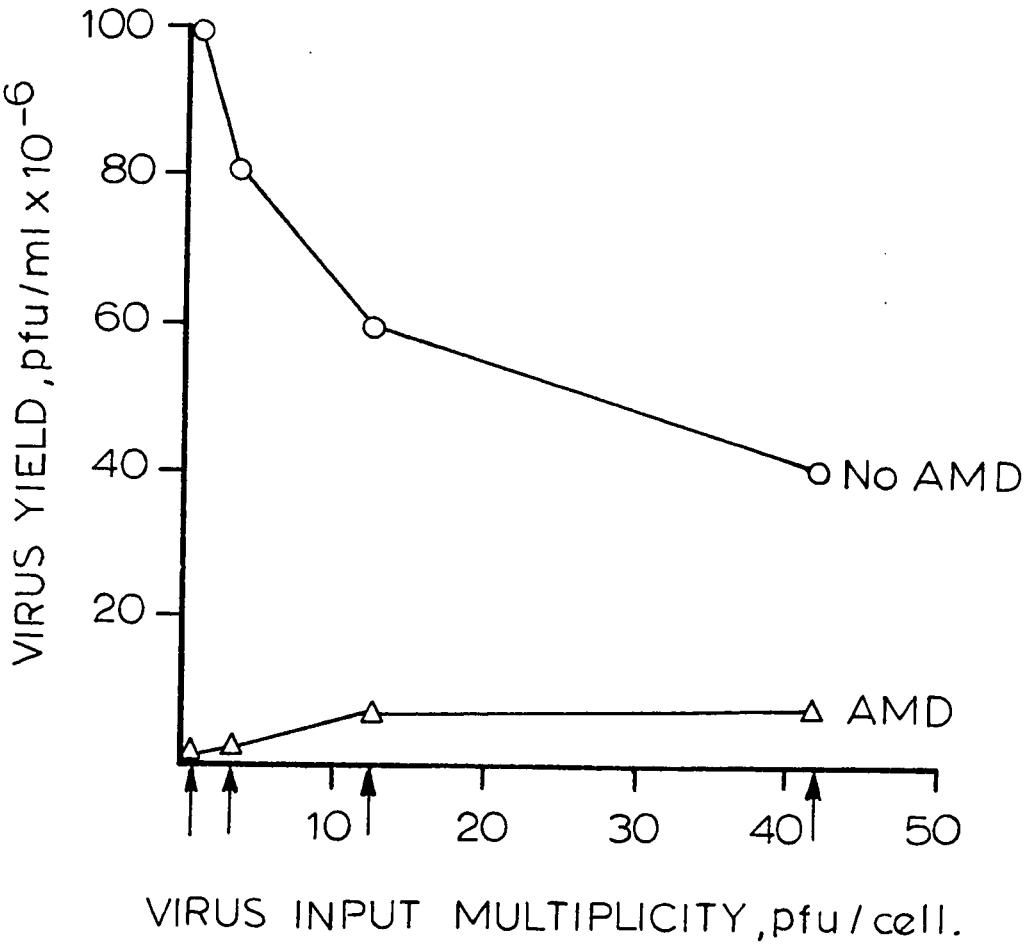
100
80
60
40
20
VIRUS YIELD, pfu/ml x 10⁻⁶
No AMD
AMD
10
20
30
40
50
VIRUS INPUT MULTIPLICITY, pfu / cell.

Discussion and Conclusions

We have obtained evidence from our dose response data that the replication of 229E virus in L 132 cells is inhibited by the antimetabolite Actinomycin D. As the primary site of AMD action is on DNA-dependent RNA synthesis (Reich et al., 1961), and since there is no DNA intermediate in the coronavirus replicative pathway (as evidenced by the lack of sensitivity of this group to DNA inhibitors--reviewed in McIntosh, 1974), the implication of finding AMD sensitivity would be that a function of the host genome is involved in the replication of this virus.

The companion curves in these experiments lend support to this finding in various aspects. Vesicular stomatitis virus (VSV) was able to replicate normally in the presence of 10 to 100 times the 50% inhibiting dose for 229E, indicating that the AMD treated cells were not incapable of supporting virus replication. In this context, it should be noted that VSV is independent of nuclear function as demonstrated by its resistance to AMD (Black and Brown, 1968) and its ability to replicate in enucleate cytoplasm (Follett et al., 1974; Wiktor and Koprowski, 1974). Similarly, the data on adenovirus inhibition and the reduction in cellular incorporation of tritiated uridine demonstrate the susceptibility of two known AMD-sensitive reactions under circumstances similar to those under which 229E virus was affected by the drug. Taken together, these evidences were accepted as supporting a hypothesis that

Actinomycin D was specifically inhibiting the replication of 229E.

The mechanism of action of Actinomycin D on the multiplication of RNA viruses is by no means clear. From the scheme presented by Baltimore (1971) it can be appreciated that there is no logical requisite for the participation of DNA in the pathway for any but the oncornaviruses; however there are numerous reports revealing AMD sensitivity in RNA viruses, leading one to hypothesize that these viruses require a host-DNA-dependent step in their replicative cycle. Without specific evidence, the host function involved could participate in any stage of the replicative cycle of these viruses, either directly, by providing a component which participates enzymatically in viral synthesis, or indirectly in the sense of providing or maintaining a specific site for replicative functions.

Viral dependence on host directed maintenance of an essential site has been alluded to by several authors investigating picornavirus replication (Cooper, 1966; Korant and Halperen, 1975) while the direct participation of host proteins has been demonstrated in the replicase of the coliphage Qβ (Kamen, 1970; Kondo et al.; 1970). By analogy ("what is true for E. coli is true for E. lephant") this pathway becomes an attractive possibility for other RNA viruses. E. coli, the host for Qβ, normally has an excess of the proteins which contribute to the viral replicase but if these proteins were virus-induced or were limiting in

concentration and unstable, then we would expect to find viral replication sensitive to AMD. In fact, some evidence has been obtained that the picornaviruses, like Qβ, may require host contribution to their replicase complexes. Cooper et al. (1971) pointed out that the portion of the poliovirus genome that was known to code for protein involved in RNA synthesis was very small, compared with the size and complexity of other known replicases and proposed a Qβ type arrangement as a possible explanation to account for both the AMD sensitivity observed and the dependence of this sensitivity on the metabolic state of the host cell as had been noted earlier (Cooper, 1966).

Regarding 229E, we do not as yet have detailed evidence which indicates a specific replicative function as being the Actinomycin target site. An examination of the effect of adding AMD at timed intervals during the growth cycle, however, revealed a temporally discrete vulnerability with the period of maximal sensitivity occupying the first one third to one half of the growth cycle. In this respect our result is similar to the situation found in members of the togavirus (Yamazaki and Notkins, 1973), picornavirus (Cooper, 1966; Black and Brown, 1968; Korant and Halperen, 1975) and myxovirus (Barry et al., 1962; Gregoriades, 1970; Pons, 1973) groups, where the production of early proteins, and interestingly, RNA replication, often appear to be the drug sensitive reactions. Whether this will also prove to be the case with 229E will have to await further

investigation.

The data obtained with increasing multiplicities would also support a hypothesis that 229E requires a limiting, unstable product of host transcription (e.g. RNA or protein). According to this concept, the necessary product would have a greater probability of participation in the viral replicative cycle when the availability of virus is increased by raising the input multiplicity. There are equally plausible alternatives, however, such as virus induction of a host function which would be correspondingly greater in the presence of greater amounts of virus. Although the present experiment leaves the mechanism of AMD action an open question, there are several practical implications. In the first place the inhibition observed varies with the input multiplicity, thus the dose-response data discussed above are not absolute, but relative to the conditions used. This is a characteristic shared with at least one other virus, poliovirus type I (Sabin), which showed the same effect in this system (unpublished results). Secondly, if further studies are conducted on the replication of 229E in AMD-treated cells, the multiplicity effect might be exploited to enhance viral functions.

The companion curve in Figure 16 suggests that a form of autoinhibition is occurring in the untreated cultures. Several mechanisms have been implicated in multiplicity inhibition of viral replication including interferon (Fenner et al., 1974) and many other factors (reviewed in

Lonberg-Holm and Philipson, 1974). The fact that AMD treated cultures permitted increasing yields of virus in spite of increasing IM favors explanations involving protein synthesis, e.g. interferon in the inoculum (which may act through stimulating cellular production of an antiviral protein, see Ho and Armstrong, 1975) but as we were diverging from our original objectives we did not pursue this phenomenon further.

III. ISOLATION AND MORPHOLOGY OF AN INTERNAL COMPONENT FROM THE VIRION

Introduction

The "large" RNA viruses (usually considered to include the paramyxoviruses, orthomyxoviruses, rhabdoviruses and oncornaviruses [e.g. Barry and Mahy, 1970; Fraenkel-Conrat and Wagner, 1975]), comprise a group with many characteristics in common. They possess a single stranded RNA genome, the virions are large, often pleomorphic particles enclosed by a fringed envelope and mature by budding through modified cellular membranes. They are similar in appearance when examined by negative staining in the electron microscope and possess a helical nucleocapsid or at least a linear nucleoprotein that might be interpreted as such (Apostolov and Flewett, 1965; Horne and Waterson, 1960; Howatson and Whitmore, 1962; Simpson and Hauser, 1966; Nowinski et al., 1970). The nucleoprotein component is occasionally seen in untreated virions but is usually better revealed by detergent or solvent disruption of the virion and can often be isolated quantitatively by such methods (Bukrinskaya, 1973).

The coronaviruses comprise a recently described virus group which shares many of the characteristics listed above (Almeida et al., 1968; Tyrrell et al., 1975).

Although the external morphology of the virion is well defined, little is known about the internal organization of the particle. Apostolov et al. (1970) reported evidence of a threadlike internal structure in thin sections of avian infectious bronchitis virus (IBV), but as yet there are no confirmatory data from negative staining or from isolation of internal components. In fact, there is little agreement as to how the nucleic acid is packaged within the envelope and several interpretations of structure have been advanced based upon data from different laboratories (McIntosh, 1974).

In view of the many similarities between coronaviruses and the other large RNA viruses it seemed reasonable to expect that an internal nucleoprotein structure could be isolated and characterized. Further support for this possibility was obtained from preliminary studies which indicated that the virion of coronavirus 229E contained an RNA-dependent RNA polymerase (Johnson-Lussenburg et al., unpublished results), an activity which has been found to be intimately associated with nucleocapsid structures in several virus groups (Chow and Simpson, 1971; Robinson, 1971; Szilagyi and Uryvayev, 1973).

The following studies report the isolation and initial characterization of a ribonucleoprotein structure from coronavirus 229E.

Materials and Methods

i) Growth of Virus

Monolayer cultures of L 132 cells in $75cm^2$ disposable culture flasks were used for virus growth. Cultures were used on the second or third day after sub-cultivation, at which time the monolayer was completed and contained 1.5 to 1.8 x 10^7 cells. Cultures were drained of growth medium and inoculated with 0.5 ml of virus, diluted to give an input multiplicity of 3-5 pfu per cell. Adsorption was allowed to proceed for 1 hour at room temperature during which time the inoculum was redistributed over the cell sheet at 15 or 20 minute intervals. Twelve ml of maintenance medium (Medium 199), containing 0.2% bovine serum albumin (BSA, Sigma Chemical Co.) as suggested by Bucknall et al. (1972), was added to each culture and they were incubated at 33^oC for 40 hours. After incubation cultures were frozen at -20^oC or -70^oC until further use. The lower temperature was chosen if extended storage periods were anticipated.

ii) Preparation of Labelled Virus

Cells were prepared and infected as above. At the end of the adsorption period, MEM with 0.2% BSA was added to the monolayers and either [5-^{3}H]-uridine (10 µCi/ml; sp. act. 28 Ci/mmole, New England Nuclear) or both ^{3}H uridine as above and a ^{14}C amino acid mixture (1 µCi/ml;

New England Nuclear, Cat. No. NEC 445) were included in the maintenance medium. Incubation and subsequent treatment were as for unlabelled virus.

iii) Virus Harvest

Preliminary experiments indicated that 75 to 90% of the virus was cell associated under the conditions employed for growth (Table 11), therefore virus was harvested by subjecting the monolayers to 3 freeze-thaw cycles to aid in virus release. The resulting whole culture lysates were clarified by centrifugation at low speed in an IEC PR6 centrifuge at 2000 rpm for 20 minutes at $4^{o}C$. This step did not affect virus titres appreciably, but subsequent manipulations were attended by an inevitable loss of infectivity.

iv) Preliminary Concentration

Initial concentration of the virus was accomplished by ultracentrifugation. In early experiments this was done by simple pelleting in the ultracentrifuge, but the recovery of infectivity in the resuspended pellet was low, and most of this activity could be removed by subsequent low speed centrifugation. In later preparations, the virus was centrifuged onto a sucrose cushion. Clarified whole culture lysates were centrifuged at 48,000 g for 60 minutes at $10^{o}C$ in the Beckman Spinco SW 25.2 rotor over a cushion containing 7 ml of 65% $^{w}/_{v}$ sucrose. After centrifugation,

TABLE 11

VIRUS DISTRIBUTION IN CULTURE SUPERNATANT AND WHOLE CULTURE LYSATES

Maintenance Medium	Virus Titre, pfu/ml		Proportion of Virus in Supernatant
	Culture SNF*	Whole Culture**	
199 alone	1.2×10^7	4.8×10^7	25%
199/2% FCS	1.4×10^7	9.2×10^7	15%
199/0.2% BSA	1.0×10^7	1.2×10^8	8.3%

* Culture supernatant fluid sampled before freeze-thaw procedure.

** Cells and supernatant after 3 freeze-thaw cycles.

an opalescent band was visible at the interface; these bands were collected in 4 ml per tube by tube bottom puncture and were found to contain an average of 53% of the infectivity present in the starting lysate.

The virus, present as a twelve-fold concentrate in a mixture of maintenance medium and sucrose, was further concentrated and washed free of sucrose by ultrafiltration using the XM 300 membrane in an Amicon model UF 52 cell under nitrogen pressure in a cold room. Since the virus bands contained about 40% sucrose, successive washings with 0.001M phosphate buffer, pH 7.2, were required to reduce the concentration to 2% or less.

v) Density Gradient Centrifugation

Gradients were prepared in cellulose nitrate tubes supplied by Beckman for the 25.2 rotor. The tube capacity was 60 ml, and gradients were prepared in 6 steps of 9.3 ml each from 10, 15, 20, 25, 30 and 35% w/w sucrose (Schwartz-Mann, density gradient grade), giving a total volume of 55.8 ml per tube. After formation of the step gradients, they were refrigerated overnight at 4^{o}C to allow diffusion to linearity. The gradient shape was chosen so that virus sedimentation could not be density-inhibited, yet a good separation from non-viral components could be expected (Anderson et al., 1966).

Gradients were overlayered with 2 ml of virus concentrate per tube and immediately run at 63,000 g for 90

minutes at 10°C after which 2 ml aliquots were collected through a tube bottom puncture. Sucrose concentrations in the fractions were determined in a refractometer (Erma Optical Works, Ltd., Tokyo). The position of the virus band was first determined by infectivity assay; in later runs [5-^{3}H]-uridine labelled virus was incorporated into each virus batch or a portion thereof, and the peak of uridine activity was located by liquid scintillation counting (LSC) of small aliquots from each fraction. The cocktail used for these specimens was composed of BBS-3, 100 ml; butyl-PBD, 8 g (both from Beckman Instruments, Inc.); water, 50 ml and toluene to 1 litre (Newman, 1973).

Steeper gradients were used for subsequent isopycnic banding of virus and for the separation of internal component from whole virus. These were also prepared manually, using 9/16 x 3½ inch cellulose nitrate tubes obtained from Beckman for the SW 41 rotor. Concentration steps of 25, 35, 45, 55, 65 and 75% w/w sucrose were used, 2 ml per step and the gradients were allowed to diffuse to linearity. 0.5 ml sample volumes were applied to these gradients. Running conditions were variable, and are referred to in the text. 0.5 ml fractions were collected by tube bottom puncture for subsequent analysis.

Sucrose solutions, with the exception noted below, were prepared from a 66% w/w working stock and diluted according to a curve supplied by Beckman (reproduced in Griffith, 1975). Buffers, reducing agents and other

additives were added as required as a portion of the diluent. Since sucrose is supersaturated at 75% at room temperature, fresh solutions were required for each experiment and prepared by dissolution in a boiling water bath. Although crystallization was inevitable when this concentrate was stored at room temperature, we were able to use 25-75% gradients in runs as long as 40 hours. Visible crystalization was encountered in only 1 run, where it had proceeded so far as to be just barely visible at the end of the run.

vi) Electron Microscopy

Most investigations were done using the negative staining technique of Brenner and Horne (1959). 2% phosphotungstic acid was prepared in distilled water and adjusted to a final pH of between 6 and 7.5 with 1 N NaOH; generally pH 6.5 produced the best results. As Bradley (1962) had demonstrated that other heavy metal salts might reveal different aspects of virus structure, 2% uranyl acetate and 2% ammonium molybdate were also used in investigating the structure of the isolated subviral components.

Specimens were prepared for microscopy by several methods; one such method was similar to that described by Howatson (1969). Using finely drawn pasteur pipettes, preparations were placed directly onto carbon stabilized, Formvar coated grids and allowed to adsorb for 1 minute.

Excess sample was drained by touching filter paper to the edge of the grid and the grid was then usually washed twice with distilled water, again draining the excess with filter paper. The staining solution was then applied to the grid, allowed to remain for 30 to 60 seconds, drained as above and the grid was allowed to air dry.

In a second method, material to be examined was diluted in 0.001 M phosphate buffer and centrifuged at 91,000 g for 60 minutes. Resulting pellets were resuspended in distilled water, a droplet was applied to the grid, mixed with stain in situ, the excess was drained off and the grid allowed to air dry.

Grids were also prepared using the agar diffusion method described by Anderson and Doane (1972), which was found to produce acceptable specimens from a variety of solutions. Many samples of interest contained high concentrations of sucrose which drew liquid from the agar unless it was previously dried slightly; furthermore, probably due to the nature of the samples being applied, it was found that a better quality of grid was obtained if the specimen and grid were left on the agar surface in a covered dish overnight at $4^{o}C$ before staining.

Once prepared, grids were examined immediately in the EM or stored in a desiccator until they could be screened. All examinations were done in a Philips EM 300 electron microscope.

vii) Isolation of Viral Ribonucleoprotein

For isolation of nucleoprotein, we used a method taken from that described by Davis and Rueckert (1972) for the isolation of Rous sarcoma virus (RSV) nucleoprotein. Tris-EDTA buffer was prepared as a stock 1M in Tris ("Trizma" brand of tris-(hydroxymethyl)-aminomethane, Sigma Chemical Co.), 0.1 M in EDTA (disodium ethylenediaminetetracetate, A.C.S., Fisher Scientific) adjusted with HCl to give a pH of 7.2 at 1/100 dilution. Dithiothreitol (DTT, Sigma) was freshly prepared as a 10% solution in deionized water and Nonidet P-40 (NP40, Shell Chemicals Co.) was similarly prepared as a 2.5% solution. A reaction mixture for virus disruption was prepared from the above ingredients to contain 0.5% NP40, 2% DTT and 1/50 of Tris-EDTA buffer. To this mixture, at ice bath temperature, was added an equal volume of freshly purified virus in 0.001 M phosphate buffer, and the mixture was immediately layered onto various preformed, precooled sucrose gradients containing 0.4% DTT and 1/100 dilution of Tris-EDTA buffer. Untreated virus was mixed with an equal volume of 0.001 M phosphate buffer and run in parallel on phosphate buffered sucrose gradients to serve as a control. All virus preparations were a mixture of unlabelled virus together with sufficient labelled material to give an overall level of label that could conveniently be detected by LSC.

Gradients were fractionated as described above. Aliquots were taken for LSC into the cocktail also described

above and counted ([5-^{3}H]-uridine label) in a Beckman LS-250 scintillation counter using a wide tritium window. Doubly labelled virus was counted in a Nuclear Chicago Isocap/300 liquid scintillation counter (courtesy Dr. Peter Anderson) programmed for simultaneous counting of both isotopes. Resultant raw counts were corrected for background and spillover before plotting.

Grids were made from sucrose gradient fractions and examined in the electron microscope by methods already described.

Infectivity assays were done by the plaquing technique outlined in a previous section. Dilutions of gradient fractions were made in MEM with 10% FCS and/or the diluent described by Szilagyi and Uryvayev (1973) for the titration of infectivity of VSV ribonucleoprotein. This diluent was prepared from powdered phosphate buffered saline mixture (Dulbecco's Grand Island Biological Co.) to which DEAE-dextran was added to a concentration of 800 µg/ml, DTT to 3.5 mM (0.54%), glycerol (Harleco) to 5% and FCS to 0.5%.

viii) Calculation of Sedimentation Coefficients

Sedimentation coefficients for whole virus and subviral component were estimated using calculations based on the method of McEwen (1967). In the original description of this method, two quantities appear to be somewhat arbitrary: the value used for starting sucrose

concentration (z_1) was adjusted downward in the sample calculation without the method or criteria being specified; secondly, the value used for starting radius (r_1) was not defined as to whether it was taken from the top of the centrifuge tube, mid sample, or the top of the gradient--appreciable differences in the hypothetical sucrose concentration at the axis of rotation (z_0), as well as in the calculated sedimentation coefficient (S) result, depending on which radius is chosen as a basis for calculation. This effect is especially pronounced when using steeper gradients, large sample volumes or less than full tubes.

To resolve these difficulties, a graph was prepared depicting the relationship between volume sampled and radius from centre of rotation. Data for this plot were obtained from measurements of liquid height in rotor tubes as a function of volume, then converting these data to radial distances from the manufacturer's specifications for the rotor concerned. On the same graph, sucrose concentration was plotted against radius; the data for this curve were obtained from measurements on the positions of the interfaces between adjacent sucrose concentrations when the gradients were set up stepwise, converting these to radial distances as above, and plotting these radii at sucrose concentrations intermediate between that above and that below the interface. This second plot, % sucrose versus radius, was confirmed by refractometry on samples

from a gradient run and found to be a good representation of the distribution. Extrapolation of this curve to zero radius gave a value for z_0 which was used in subsequent calculations. The starting concentration, z_1, was also obtained from the graph, using the radius at the middle of the sample volume. Figure 17 is an example of the type of graph described.

In performing the calculations, z_2, the sucrose concentration to which the species under observation had migrated, was obtained directly by refractometry. Alternatively, taking the middle of the peak fraction as the position of the species, z_2 could be obtained from the plot referred to above. The latter alternative is advantageous when containment of the sample is desirable. The remaining calculations were done according to McEwen's equations.

Results

i) Growth of Virus

The conditions described for the growth of virus were chosen arbitrarily, having given consideration to the growth curves published for 229E in Wl-38 cells (Hamre et al., 1967) and in L 132 cultures (Bradburne and Tyrrell, 1969). Yields of virus obtained were generally of the order of 200-300 pfu per cell when titrated after harvesting by 3 freeze-thaw cycles.

Since the growth curve data obtained in tube cultures (see previous section) indicated that virus titres

FIGURE 17

Figure 17:- Standard curve used in calculation of sedimentation coefficients. Sucrose concentration-and-volume versus radius plot for 10%-35% sucrose gradients in the SW 25.2 rotor, as used in the calculation of sedimentation coefficients (details in text).

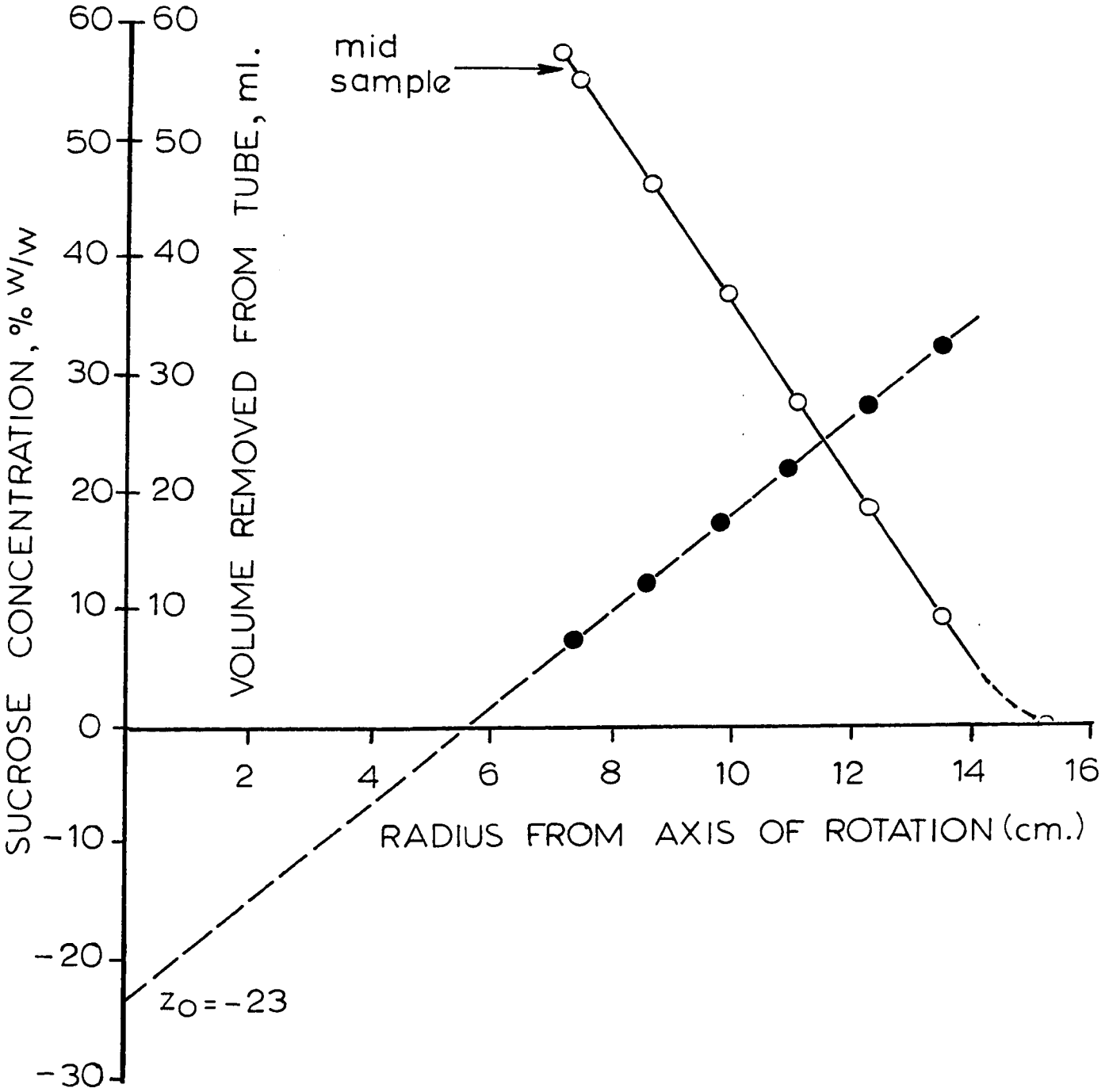
60
50
40
30
20
10
0
-10
-20
-30
SUCROSE CONCENTRATION, % W/W
VOLUME REMOVED FROM TUBE, ml.
mid sample
2
4
6
8
10
12
14
16
RADIUS FROM AXIS OF ROTATION (cm.)
$z_o = -23$

reached a maximum at around 24 hours after infection at high multiplicity, and since human coronaviruses appear to be temperature labile (Bradburne and Tyrrell, 1971; Bucknall et al., 1972), it was thought that greater yields might be obtained from flask cultures infected at higher multiplicity and incubated for shorter times (i.e. 24 hours). On three separate occasions, groups of flasks were inoculated at an input multiplicity of 20 (assuming approximately $2x10^7$ cells per flask), and incubated for 24 to 29 hours at 33°C. No increased yield was found, as titres obtained on freeze-thawed pools for these batches indicated that 306, 190 and 212 pfu of virus were produced per cell in the three preparations, similar yields to those obtained in the routine method; 200-300 pfu per cell thus appeared as a practical limit in our hands.

ii) Purification

Preliminary experiments had indicated that 229E sedimented in sucrose gradients as a sharp peak (determined by infectivity assay). Virus grown in the presence of [5-^{3}H]-uridine and centrifuged under the same conditions showed a similar peak of ^{3}H activity in the same region and when fractions from these gradients were assayed for both virus and tritium, it was found that their peak distributions in this region of the gradient were exactly coincident (Figure 18). Since [5-^{3}H]-uridine is incorporated specifically into RNA, this result provided additional evidence that the

FIGURE 18

Figure 18:- Distribution of ^{3}H label and infectivity in 10%-35% sucrose gradient after rate zonal centrifugation of HCV/229E grown in the presence of tritiated uridine. Note the coincident peaks centred on fraction 14.

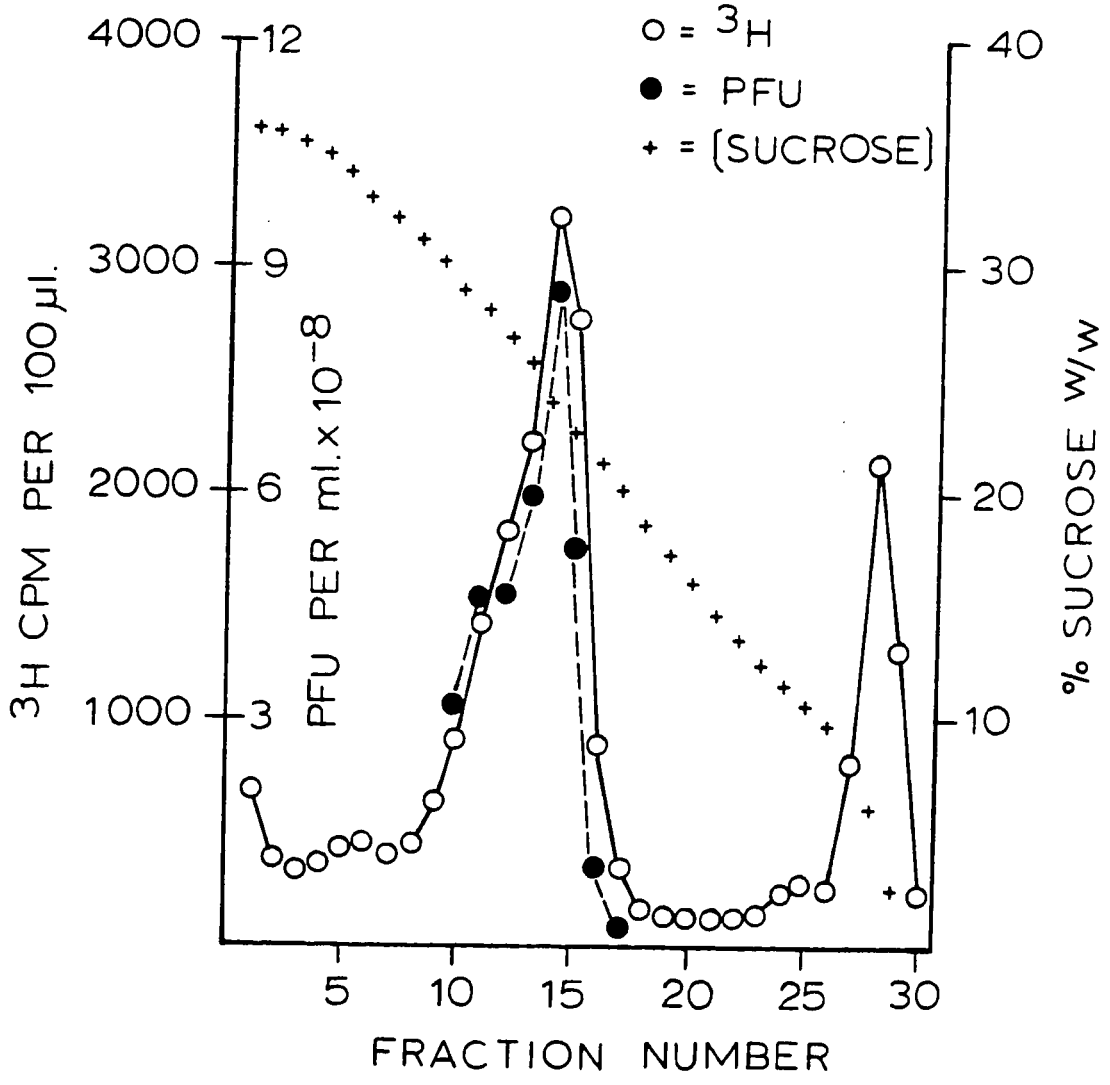
o = 3H
● = PFU
+ = (SUCROSE)
4000
3000
2000
1000
12
9
6
3
40
30
20
10
3H CPM PER 100 µl.
PFU PER ml. x 10-8
% SUCROSE W/W
5
10
15
20
25
30
FRACTION NUMBER

genome of 229E was RNA. Technically, the use of tritium label as a tracer for following the distribution of virus in these gradients eliminated the cumbersome infectivity assay requirement, allowing the virus band to be located by scintillation counting in a matter of minutes.

In the curve presented in Figure 18, the label remaining at the top of the tube (fractions 27-30) is reduced compared to most runs, where the amount remaining on top of the gradient exceeded that recovered in the virus peak. In collecting the cushioned virus which was put on this gradient, very little of the maintenance medium was included; in routine practice the cushioned sample contained more of the supernatant and the corresponding gradients contained more soluble label.

The virus peak itself is well resolved in the sense that no other uridine containing peaks are nearby, but the fractions toward the tube bottom (i.e. lower numbered) are elevated to about 10% of peak height. This was a frequent finding and might represent aggregated virus which would be expected to migrate faster than the rest. It will also be noticed that there is a slight irregularity in the "downstream" side of the peak, i.e. in fractions 10-14; this was frequently observed and was often more pronounced, taking the form of the shoulder seen in the plaque assay data. It was thought that this might be indicative of two classes of virus similar to the light and heavy forms of IBV reported by Bingham (1975), but none of our gradients resolved this

feature. The shape of the virus peak is reproducible and samples taken for virus recovery included five fractions: the peak fraction itself, the three immediately below it in the gradient and the one immediately above it.

In preparing virus for disruption studies, these gradient fractions were pooled, washed with 0.001 M phosphate buffer and concentrated by ultrafiltration. Data are presented in Table 12 from 9 experiments in which virus was purified to this stage and concentrated by a factor of approximately 150 with respect to starting volume. These data indicate that the final yield in terms of infectivity is somewhat variable, 5-27% of the amount initially present; and secondly they indicate that specific infectivities as high as 4.5×10^{10} pfu/mg of protein have been obtained by this method.

Sedimentation coefficients calculated from preparative runs done under several different conditions are shown in Table 13, which lists representative data. Most gradients were run as for number 4 and 5, yielding an S value of 390 as in number 4. Runs 4 and 5 differed in position of peak by ½ fraction, yet the calculated sedimentation coefficients differ by about 20% (100 x difference/mean). This is a characteristic of the tables used in performing the calculations, which are plotted in steps of 2% with respect to sucrose concentration: under the conditions used here a large difference in S value results from a difference of one step. Thus, the tables would

TABLE 12

RECOVERY OF VIRUS AFTER RATE ZONAL CENTRIFUGATION

Run Number	Total pfu at Start x 10^{-8}		Concentrate After Gradient Centrifugation			
	Lysate	Clarified	Total pfu ($\times 10^{-8}$)	µg Prot.**	S.I.***	Yield %
C-1	-*	22	3.6	130	27.7	16
C-2	-	450	3.0	70	42.9	6.7
C-3	-	-	13.8	118	117	-
C-4	65	-	40	80	50	6.2
C-5	-	-	0.54	116	4.7	-
C-6	540	-	144	320	450	27
C-7	240	-	13	-	-	5.4
C-9	380	-	50	-	-	13

* Data not available.

** Protein estimations were done by the technique of Lowry et al. (1951).

*** Specific infectivity, pfu/mg protein, x 10^{-8}.

TABLE 13

SEDIMENTATION COEFFICIENT OF 229E

Run Number	Rotor Model	Gradient % Sucrose	Duration (Minutes)	Speed ($rpm \times 10^{-3}$)	Peak % Sucrose	Sedimentation Coefficient
1	SW-41	15-40	80	30	28.3(28)*	495
2	SW-25.2	10-35	60	20	17.3(18)	472
3	SW-25.2	10-35	75	22.5	20.4(20)	378
4	SW-25.2	10-35	90	22.5	21.6(22)	390
5	SW-25.2	10-35	90	22.5	23.1(24)	476

* Number in parentheses used for calculation.

accurately predict the position of a particle of known sedimentation rate, which they were designed to do, but are less accurate in determining S values from experimental data. The variation in Table 13 could therefore result from very minor variations in experimental data and sedimentation coefficients calculated by this method must be regarded as approximations.

Electron microscopy of the purified virus concentrates revealed large numbers of typical coronavirus particles, with membranous debris being the major contaminant. Centrifugation of this material for longer periods in steeper gradients (see below) gave rise to the formation of two visible bands, the heavier of which (density 1.19) contained the uridine label and typical virions while the lighter fraction was largely membranous debris with occasional adsorbed virions.

iii) Electron Microscopy of Disrupted Virus

Rate-zonal purified virus in 0.001 M phosphate buffer was disrupted under a variety of treatments and examined in the electron microscope. Three classes of method were used; treatment with detergents, treatment with solvents and simple storage in phosphate buffer and all led to the breakdown of virus particles. When examined by electron microscopy, disrupted virions appeared to contain an amorphous matrix which either represented the internal component, or else obscured any other structure which may

have been present (Figure 19A). On many grids, particles could be found with minimal morphological damage. These appeared as intact virions but the envelopes of which had been breached sufficiently to allow penetration of stain. The interior of these particles similarly appeared featureless (Figure 19B).

In many preparations a new structure could be found external to the virions which appeared highly significant even though its relationship to the whole particle was not explicit. This is illustrated by the following observation.

> . . . virions with typical coronavirus morphology were found in fresh preparations (Figure 20A). However, after the purified preparations in 0.001 M phosphate buffer had been stored overnight at 4°C fewer typical virions were evident and disrupted or disintegrating forms were seen (Figure 20B). Many particles appeared to have lost only their petal-like projections (peplomers), but in addition, there were discrete tangles of threadlike strands which were 8-9 nm in width and appeared to be continuous. The possibility that these strands might be released internal component is supported by Figure 20C in which the same strands appear to be released from a collapsing virion.[1]

iv) Isolation of Virus Ribonucleoprotein

Preparations of virus containing ^{3}H-uridine labelled 229E were purified by velocity gradient centrifugation, then treated with NP40. In preliminary experiments the resulting material was immediately layered onto a 15-25% w/w sucrose gradient containing Tris-EDTA buffer and DTT above a 65% w/v

---

[1]Quoted from Kennedy and Johnson-Lussenburg, 1976.

FIGURE 19

Figure 19:- Two virions whose envelopes have been disrupted (A) or sufficiently compromised as to allow penetration of stain (B). The virus preparation depicted in A had been stored in 0.001 M phosphate buffer at $4^{o}C$ for 7 days, while B was taken from freshly prepared virus which had been exposed to amyl acetate on the grid. Typically, no details of internal structure can be seen within the viral envelopes. Bar represents 100 nm.

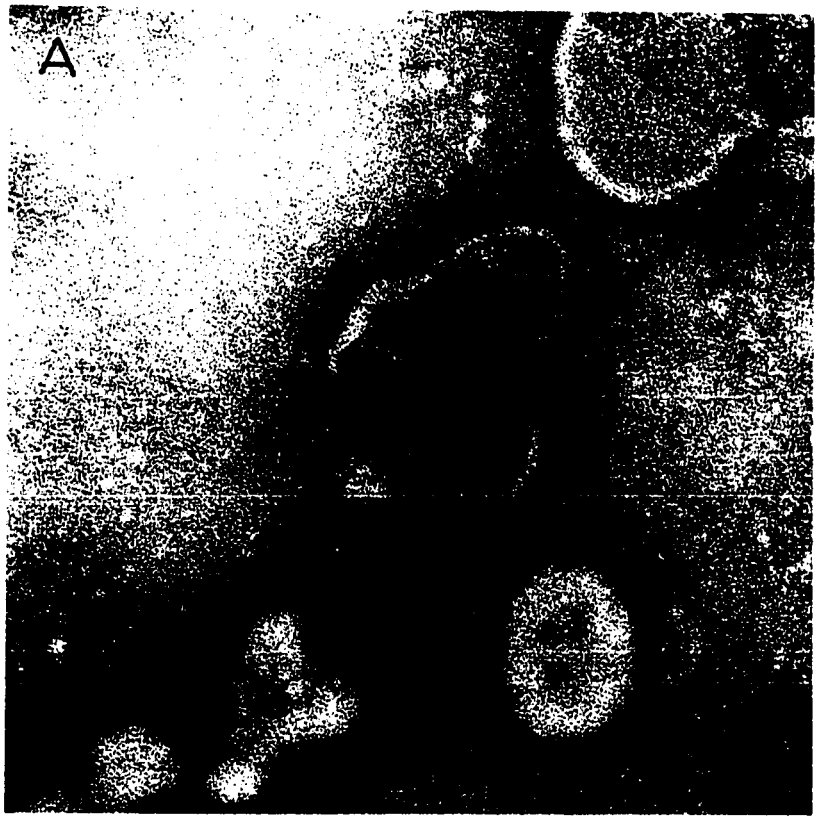
A

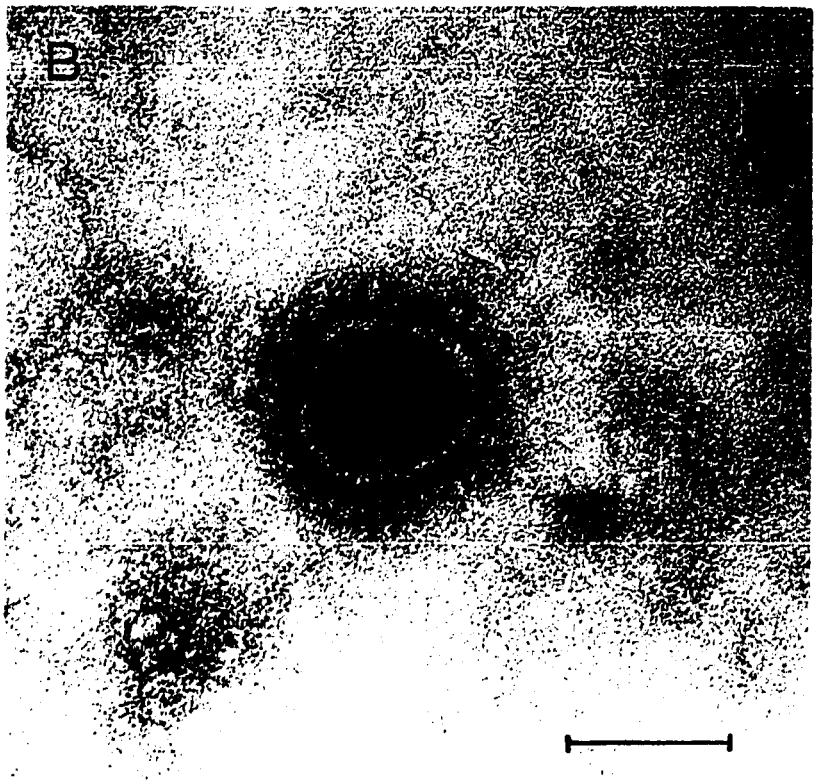
B

FIGURE 20

Figure 20:- A. Freshly prepared virus. Morphology is typical of the Coronaviridae. B. Particles in three stages of disruption, seen after 24-hour storage at 4^{o}; upper right particle without petal-like projections is typical of many; upper left shows particle apparently losing internal component, but no structural detail is evident; bottom center shows typical discrete tangle of threadlike strands, 8-9 nm in diameter. C. Preparation as in B, showing particle releasing filamentous material. Bars represent 100 nm in all micrographs.

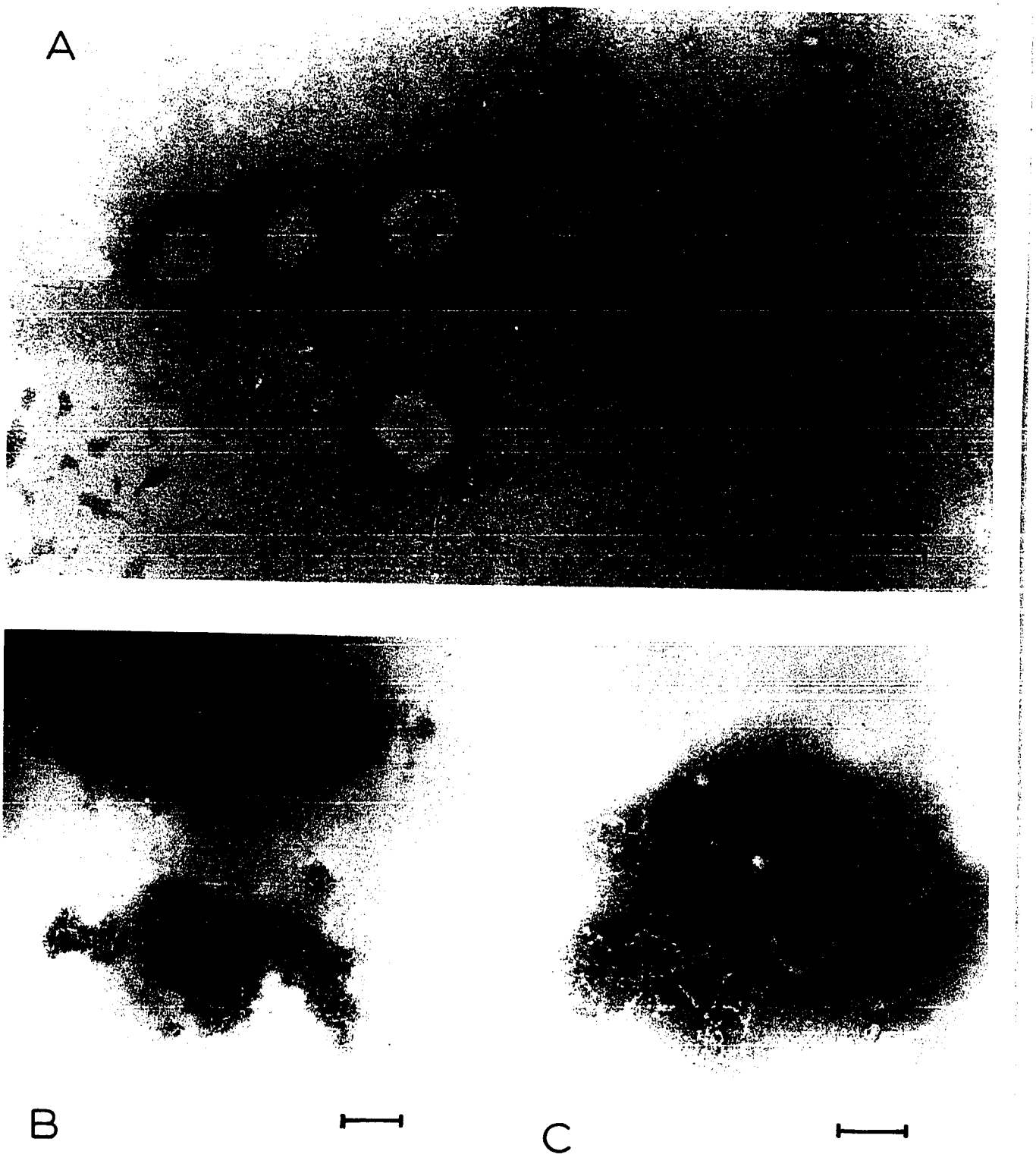
A
B
C

sucrose cushion and centrifuged at 110,000 g for 90 minutes. Untreated, but ^{3}H-uridine labelled 229E was centrifuged in parallel. Analysis of the resulting fractions revealed no difference in the distribution of ^{3}H activity of either the untreated or the NP40-treated virus, and in both cases only a single major peak was revealed which had sedimented through three-fifths of the gradients. The peak in the NP40 tubes did occur one or two fractions closer to the tube bottom than the peak in the controls but this finding in itself was of uncertain significance as replicate preparative gradients were found to differ by this much from run to run.

This similarity was difficult to reconcile with the obvious differences in appearance of the untreated versus NP40-treated virus in the EM, so it was decided to examine the two types of preparation for differences in density. When experiments were carried out using 25% to 75% w/w sucrose gradients centrifuged at 170,000 g for 15-22 hours at 10^{o}C, a clear difference could be shown between detergent-treated and untreated virus. Figure 21 gives the distribution of ^{3}H-uridine label in a control tube from such an experiment while Figure 22 was prepared using data from a tube in the same run which contained NP40-treated virus. The virus peak is located at a sucrose concentration corresponding to a density of 1.19, the peak in the NP40 tube corresponds to a density of 1.27. In either case there is a single sharp peak, indicative of a homogenous uridine-containing species, which differs in the two situations.

FIGURE 21

Figure 21:- Distribution of ^{3}H in 25-75% w/w sucrose gradient after centrifugation of ^{3}H-uridine labelled 229E at 170,000 g for 22 hours.

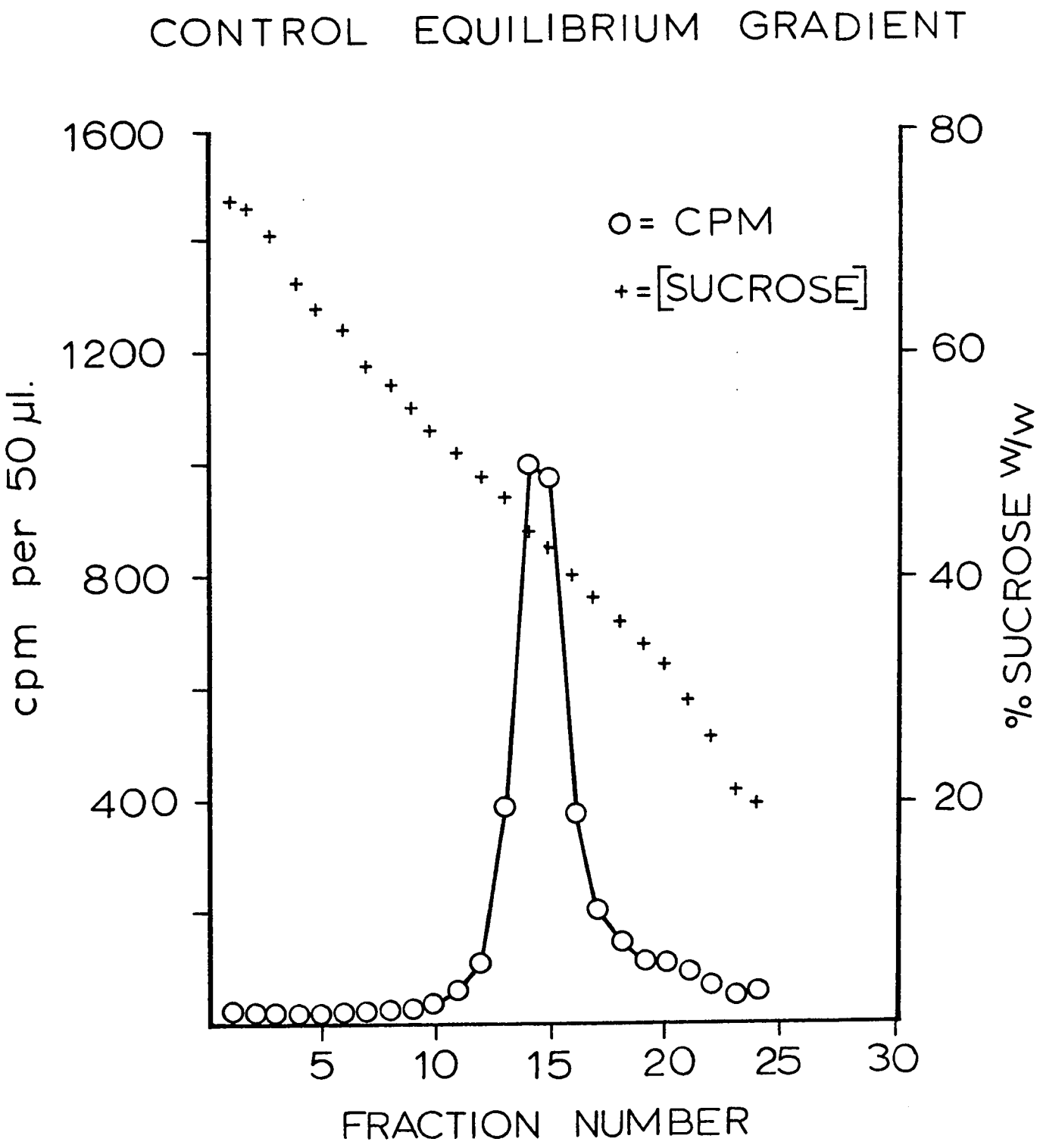
CONTROL EQUILIBRIUM GRADIENT
1600
1200
800
400
80
60
40
20
o = CPM
+ = [SUCROSE]
cpm per 50 µl.
% SUCROSE W/W
5
10
15
20
25
30
FRACTION NUMBER

FIGURE 22

Figure 22:- Distribution of ^{3}H in 25-75% w/w sucrose gradient after NP-40 treatment and centrifugation of ^{3}H-uridine labelled 229E at 170,000 g for 22 hours.

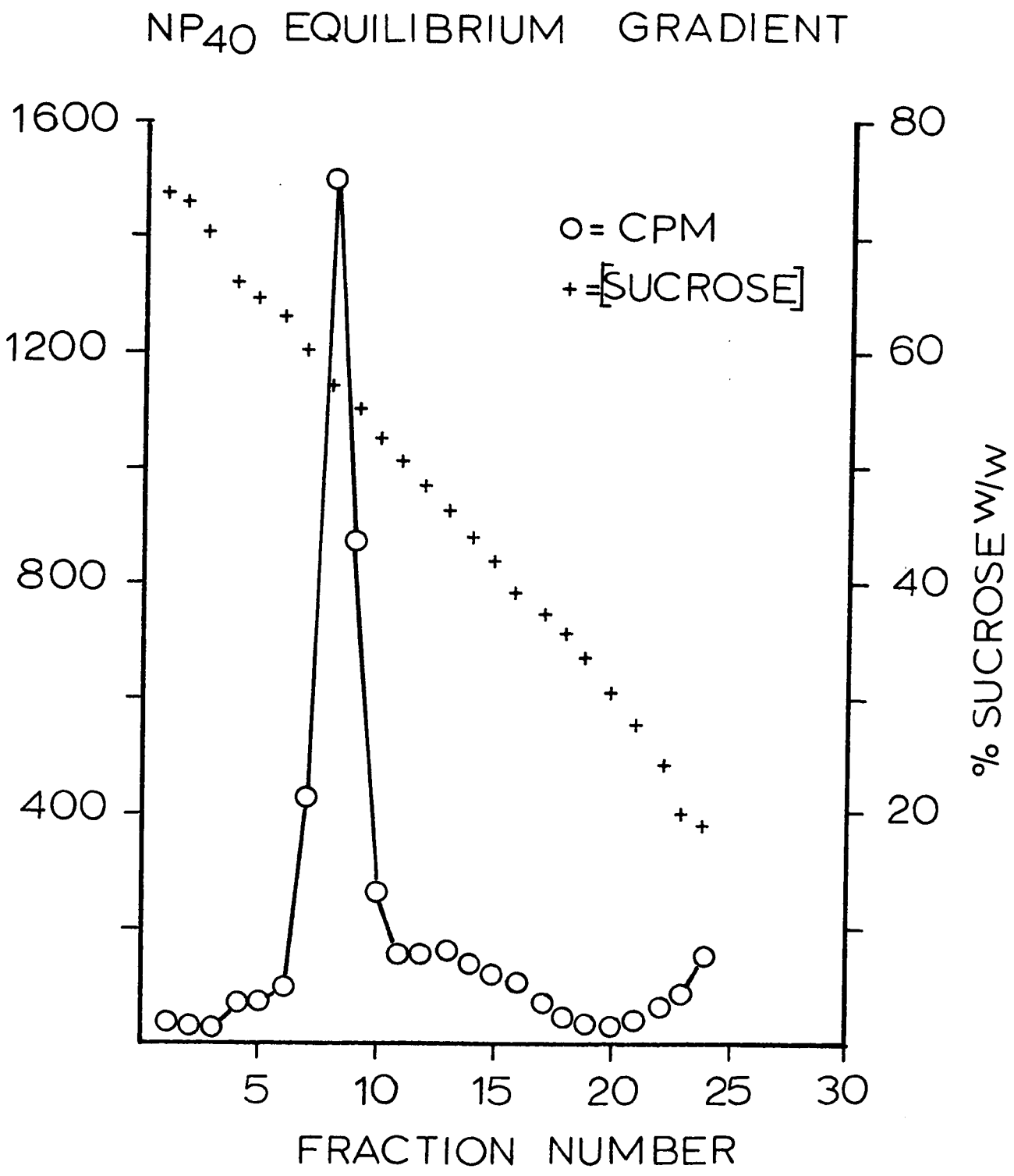
NP40 EQUILIBRIUM GRADIENT
1600
1200
800
400
80
60
40
20
o = CPM
+ = [SUCROSE]
% SUCROSE W/W
5
10
15
20
25
30
FRACTION NUMBER

It is thought that these densities are isopycnic for virus and subviral component since nearly identical results were obtained under different conditions of centrifugation:

1) Nonidet P-40 treated, ^{3}H-uridine labelled virus and labelled, untreated virus were applied to 25-75% w/w sucrose gradients and centrifuged at 110,000 g for 20 hours at 10°C. At this time, tubes were removed for fractionation, the rotor was restarted and run at 75-80,000 g for a further 18 hours after which the remaining tubes were sampled. The peak in the control tubes occurred in the same fraction from the gradients sampled after 20 hours and 38 hours. The peak in the NP40 tubes had sharpened slightly and shifted one fraction downwards after the additional 18 hours. One fraction corresponds to a change in density of 0.01 g/cm^{3}.
2) Several large preparations of virus were made in this laboratory by combining pools of rate-zonal purified virus. Individual lots were frozen in 0.001 M phosphate buffer until several had been accumulated; then they were thawed, pooled and run on 10-65% w/w gradients at 170,000 g for 20 hours at 10°C. In addition to the major, virus containing peak at density 1.19, a secondary, heavier uridine labelled peak was seen at 1.26

to 1.27. Electron microscopy of fractions from the secondary peak revealed material which appeared to be virus internal component.

3) Runs at 170,000 g in 25-75% w/w gradients for either 16 hours or 22 hours gave peaks at approximately the same density in spite of a 20% increase in run time. Virus peaks were obtained at density 1.19 and 1.20 respectively, while detergent containing tubes had peaks at 1.27 compared to 1.27 and 1.28.

While the density of 1.27 and the observations in the EM (see below) implied that the labelled RNA was associated with protein in a nucleoprotein complex, confirmation was obtained by the use of double labelled virus. 229E was grown in the presence of ^{3}H-uridine and ^{14}C amino acids and purified as before. This virus was treated with NP40 and centrifuged under reducing conditions as above. Analysis of the resulting fractions revealed that both the ^{3}H-uridine and ^{14}C amino acid activity occurred as major coincident peaks in the 1.3 density region of the gradient, demonstrating the nucleoprotein nature of this complex (Figure 23). In addition, there was a minor peak of double label activity in the 1.19 region indicating the presence of a small proportion of non-disrupted virions, while a third peak at still lower density, showing only ^{14}C activity probably consisted of detergent-released protein components.

FIGURE 23

Figure 23:- Distribution of ^{3}H and ^{14}C in 25-75% w/w sucrose gradient centrifuged at 170,000 g for 22 hours. HCV/229E was labelled with ^{3}H-uridine and ^{14}C amino acids and treated with NP-40 before centrifugation. Top of gradient is at right hand side of figure.

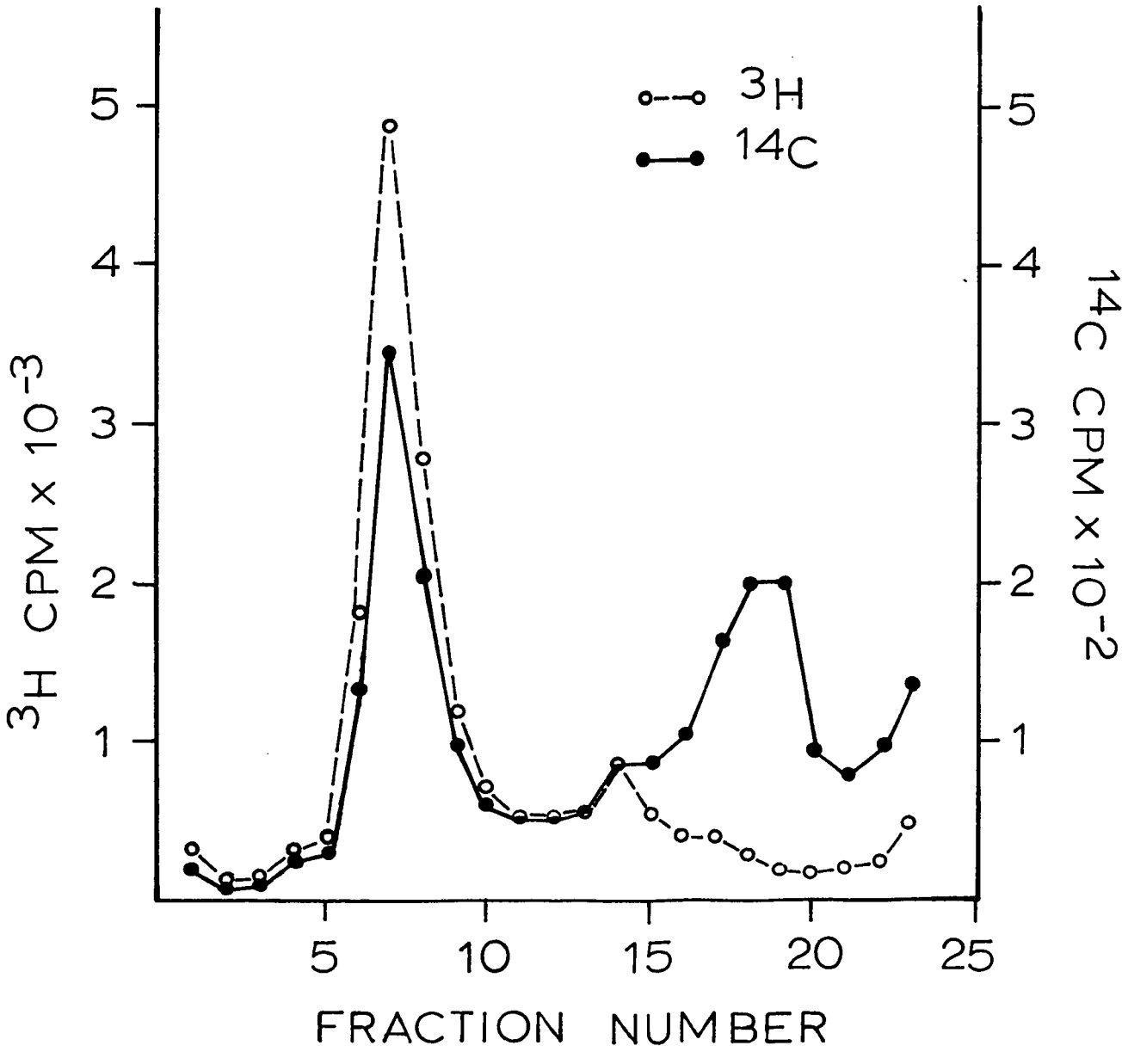
3H
14C
3H CPM x 10-3
14C CPM x 10-2
1
2
3
4
5
5
10
15
20
25
FRACTION NUMBER

Having determined the density of the new complex, 15 to 40% w/w gradients were prepared, including three with DTT and Tris-EDTA buffer and one control, to which NP40 treated and control virus were applied, respectively. Both preparations contained labelled virus. Gradients were run at 120,000 g for 80 minutes, fractionated and the peaks located by LSC. Sedimentation coefficients were calculated as before giving a value of 495 for whole virus and 457 for the nucleoprotein complex. The three replicates were identical.

v) Morphology of Isolated RNP

Grids were prepared for electron microscopy by several methods from both treated and control gradients. Samples were taken from both high density (1.27) and low density (1.19) regions after equilibrium centrifugation and were screened without reference to their origin. From these studies, it was learned that typical virions were characteristic of the low density region of control gradients, and on occasion distorted virions could be seen in this area of NP40 gradients. The other characteristic association was between a new type of particle and the high density zone of NP40 gradients. In a later study, to which we have already referred, a similar particle was seen in the 1.27 region of equilibrium gradients of untreated virus which had been stored frozen as purified suspensions. In that case, there was also a peak of uridine activity in the same

zone which probably indicated virus breakdown and spontaneous release of nucleoprotein.

The nucleoprotein particles typically had the morphology illustrated in Figure 24A, C and D. These structures were discrete with overall diameters in the range of 100 to 200 nm. Figure 24A illustrates a particle in which the linear nature of the component strand is more apparent, with some suggestion of a loosened coil arrangement being visible at one end. The strand diameter in this particle averaged 9 nm and a tracing of the visibly continuous portion led to an estimate of total length at 1.6 to 1.8 μm. This is probably an underestimate as the path of the linear structure cannot be followed with any certainty.

Other configurations were observed, but they were not so typical as those just described. Among these were more extended forms, similar to the material associated with spontaneously disrupting virions (e.g. Figure 20), and the tightly coiled structure shown in Figure 24B was also seen in one of the NP40 treated preparations. Overall coil diameter is about 66 nm while the strand diameter averages 9 nm and appears continuous over 5 turns, dissolving into amorphous, unresolved matter at each end. There is a suggestion in this micrograph and in a portion of Figure 24A that the component strand itself may be of helical construction, but this feature is not resolved in most of our micrographs.

FIGURE 24

Figure 24:- A, C and D. Typical appearance of particles seen in ^{3}H-labelled peak of gradient fractions of NP-40 treated HCV/229E preparations. B. Tightly coiled particle, also from NP-40-treated HCV/229E. There is some suggestion in A and especially B that the component strand may itself be of helical construction. Bar represents 100 nm.

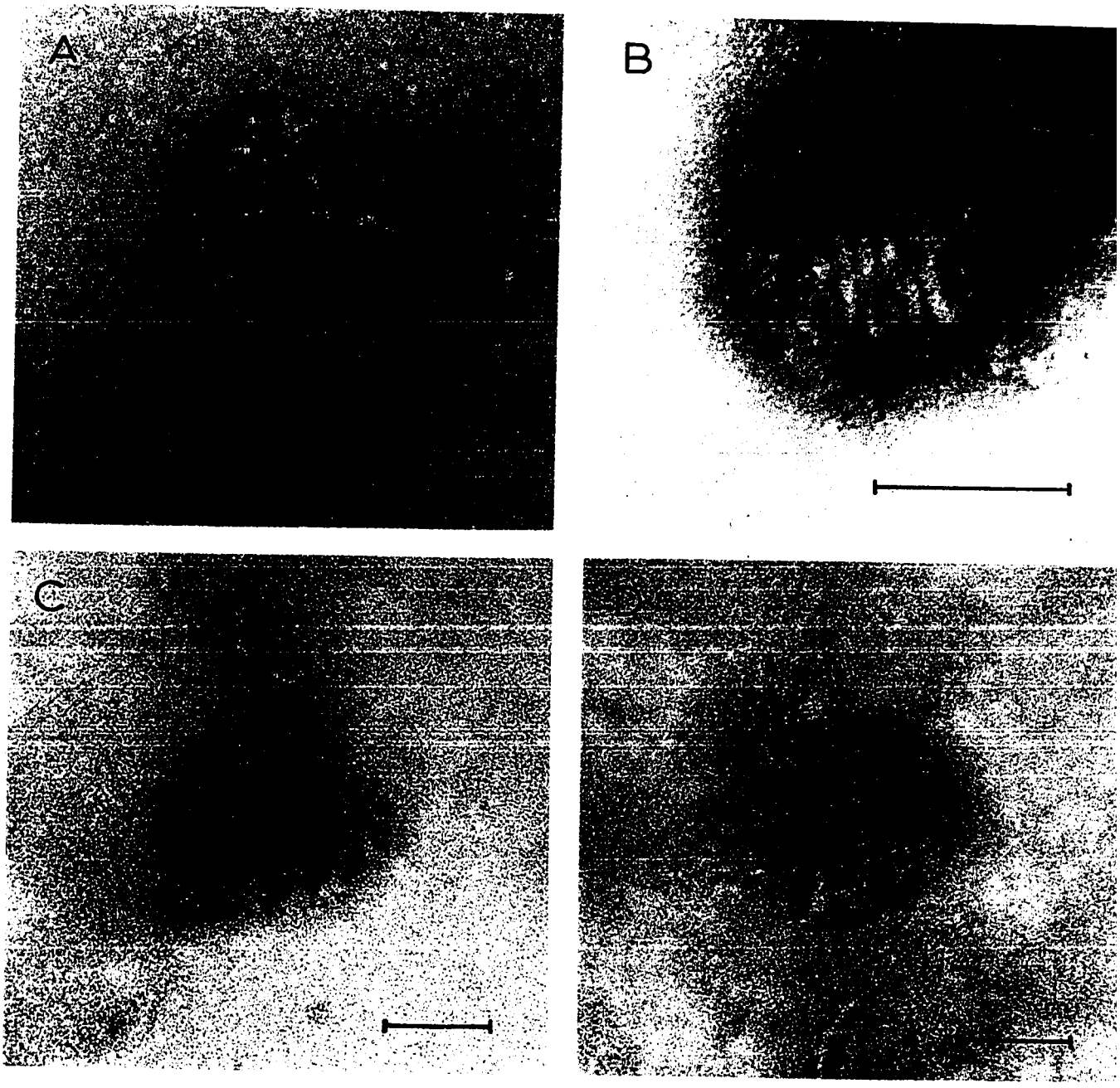
A
B
C

All of the micrographs presented were obtained using phosphotungstate negative staining. Uranyl acetate and ammonium molybdate were also employed, but no further relevant details were resolved.

vi) Infectivity of RNP

Aliquots of gradients containing NP40-treated virus were tested for infectivity on monolayers of L 132 cells, either directly or after dilution in the fluid described by Szilagyi and Uryvayev (1973). In the first trial aliquots were taken from the peak of uridine label in a rate zonal gradient and tested at tenfold dilutions from 10^{o} to 10^{-4}. Most flasks showed slight CPE after 3 days, so subcultures were made and examined after 4 days. At that time CPE was noted in the flasks receiving material which derived from 10^{-1} and 10^{-2} dilutions of the peak, but not from those representing the undiluted aliquot or those from the 10^{-3} and 10^{-4} dilutions.

A second and third attempt was made after running virus and lysate on 25/45/75% w/w sucrose discontinuous gradients. The gradients were not well chosen or standardized, but in the first of these runs (#2, Table 14), infectivity was again detected in the RNP tube and its distribution roughly paralleled the distribution of uridine label. The RNP had penetrated the 75% cushion, which was small, and which had probably diffused to considerably less than its nominal concentration, to give a "peak" at the tube bottom,

in fraction 1.

Note that again there was no infectivity detected in the undiluted material. Note too that the samples from fraction 1 in the control tube contained virus, although the peak was in fraction 17, at the 25/45 level.

In the last trial, the gradient was similar to that just described, but running time was shortened from 15 hours to 3 hours. The peak in the control tube was well defined at fraction 20, but most of the RNP appeared to be spread through the middle of the gradient, with a small peak beginning to form at fraction 3. No infectivity was demonstrated in the NP40 tube, but the control tube again showed virus near the bottom. The concentration of virus increased in fractions closer to the virus peak. When fraction 3 from the control tube was diluted in both the special diluent and in MEM, the titre was sevenfold higher in MEM.

The data described above are summarized in Table 14. The last column "Recovery of pfu" is a rough approximation.

These results must be regarded as inconclusive. The experiments were done before we had achieved a technique for clear separation of virus and RNP, and were done using small lots of virus. They are included here because they are suggestive in several respects and may aid in further studies.

TABLE 14

INFECTIVITY OF NUCLEOPROTEIN

Trial Number	Gradient	pfu (Per Tube	Treat-ment	Fraction	Dilu-uent	Plaques at Dilution 10^{o}	10^{-1}	10^{-2}	10^{-3}	10^{-4}	CPM Per 50 µl	Re-covery of pfu
1	Linear 15%-40%	$1x10^{9}$	NP40	6+7	RNPD*	-**	+	+	-	-		10^{-6}
2	Disc. 25/45/75	$4x10^{9}$	NP40	1	RNPD	0	17	3	0	ND	1694	10^{-5}
				5	RNPD	0	5	0	0	ND	273	
			Control	1	RNPD	TN***	TN	TN	ND	ND	224	
3	Disc. 25/45/75	$7x10^{9}$	NP40	1,3,5	RNPD	ND	0	0	ND	ND		$<10^{-8}$
			Control	1	RNPD	ND	48	3	0	ND	17	
				3	RNPD	TN	TN	120	12	ND	19	
				3	MEM	TN	TN	TN	86	ND		
				5	RNPD	ND	TN	TN	46	ND	26	

* RNPD = ribonucleoprotein diluent, Szilagyi and Uryvayev, 1973.

** In trial 1, dilutions were only tested for CPE on subculture.

***TN = too numerous.

It was noted that whole virus reached high sucrose densitites in the control tubes. If this is found to be the case in other gradients, then infectivity occurring in NP40 tubes, even at high sucrose concentrations, may be due to the presence of residual undisrupted virus; however, the distribution of infectivity would be expected to parallel that of the species from which it derives and therefore attempts to demonstrate infectivity should be done on several fractions in order to measure distribution in addition to simple presence or absence.

If trial 2 did, in fact, detect infectivity due to the RNP, and the parallel distributions of tritium label and pfu suggests that this might be so, then the diluent appears to aid in this demonstration by at least 170 fold, since no plaques were seen in the undiluted material from fraction 1 where 170 were expected on the basis if the titre at a 10^{-1} dilution. A similar enhancement may have been responsible for the result in trial 1.

In contrast to the apparent enhancement of RNP infectivity obtained when nucleoprotein was diluted in RNPD, this medium is deleterious to whole virus. Thus, in addition to the distribution criterion for ascribing infectivity to RNP or to residual virus, if fractions were diluted in parallel in RNPD and MEM for titration, the results could be compared on the basis of diluent effect to support distribution data.

As a general conclusion, further work should be done in such a manner as to achieve maximal separation of virus and RNP, and at higher virus loadings than we have used here since the recovery is low. Under these conditions and using the criteria suggested above, it may be possible to demonstrate an infectivity associated with isolated nucleoprotein.

Discussion and Conclusions

The growth of 229E by several protocols appeared to reach a practical limit of 200 to 300 pfu per cell. Yields of this order were obtained using different multiplicities and incubation times and in tube as well as flask cultures. In view of the observed effect of several of the plaque overlay ingredients however, it might be possible to improve on these yields, which would be an obvious asset to further analytical studies.

229E was purified by centrifugal methods to an extent that was adequate for the isolation of nucleoprotein, but it remains to be seen whether this degree of purity lends itself to more critical analysis. Specific infectivities as high as 4.5×10^{10} pfu/mg have been obtained, which compares favorably with the result of Kaye et al. (1970) who purified OC43 by adsorption-elution from erythrocytes and calcium phosphate chromatography. The latter group obtained specific infectivities of only 5×10^{9} pfu/mg and although differential losses in infectivity between

viruses and methods may reduce the value of this criterion for comparison, gradient purification techniques have proven adequate for the preparation of IBV (Bingham, 1975) and TGE (Garwes and Pocock, 1975) prior to their biochemical analysis. Incorporation of [5-^{3}H]-uridine provided a useful tracer for virus during these manipulations and in addition provided a confirmation of the nature of the genome of this virus.

Of major interest were the findings with respect to the internal component of the virus. Linear structures were seen in the electron microscope which we believe to be the viral nucleocapsid (RNP). These structures were seen in preparations of stored virus, in gradients of detergent-treated virus and in gradients of virus which had been frozen and thawed in the purified state. In the latter two cases these linear forms were found at a density of 1.27-1.28 and were correlated with peaks of labelled viral RNA. The fact that both spontaneous disruption and detergent treatment produced a particle of similar density and appearance suggests that this is a relatively stable subviral component.

The apparent linearity of this subviral strand indicates that it is probably assembled according to the principles of helical symmetry (Caspar, 1965) and, in addition, there was direct evidence in several micrographs (Figures 24A and 24B) of its helical nature. Furthermore, since coiling of the strand, as observed in nucleocapsids

of influenza virus, has been explained by Horne (1974) to be a consequence of specific bonding patterns between neighboring structural units in a helical capsid, the spring-like arrangement in Figure 24B and the traces of coiling seen in other particles constitute further evidence for the basically helical construction of this capsid.

Differences in the morphology of the RNP were observed depending on whether grids were prepared from Tris-EDTA buffered reducing gradients or from phosphate buffered gradients and solutions. In the former situation the nucleoprotein appeared slightly wider and less discrete when compared with the latter. These changes in appearance may be reflections of conformational changes in the particle produced by the chemical environment from which they were taken. If so, then it is tempting to speculate that nucleoprotein within the viral envelope may be further altered by its particular environment to the extent that it appears amorphous in the EM. Our own studies, certainly, have shown amorphous material to be characteristic of the envelope contents and similar micrographs have been obtained from detergent disrupted preparations of IBV (Berry et al., 1964) and TGE virus (Witte et al., 1968).

Remaining highly speculative for a moment, it is possible that a parallel situation is found in the case of influenza virus where a large helical structure which is occasionally seen within the virion may represent the native (undenatured) form of the viral nucleoprotein. In a recent

report, Almeida and Brand (1975) present evidence that the coil is an extremely labile configuration which may or may not be seen in preparations of disrupted virus, depending on the conditions used; but under gentle conditions this structure may be demonstrated in association with the majority of disrupted particles. A detailed examination of their micrographs suggests that even individual helices may show morphological variations along their length. For example in their Figure 2, transitions can be seen in an elongated coil from tight to diffuse or amorphous configurations and back again. Interestingly, amorphous regions appear to be associated with exudate from disrupted viral envelopes. Similarly, the same figure contains a coil being extruded through a disrupted envelope; the coil is compact in structure distally but appears to become loosened and ill-defined morphologically as one traces its course back into the envelope. Thus, one could speculate that the envelope contains a substance which interacts with the nucleoprotein and which hinders the visualization of the nucleoprotein "in situ." Removing this substance by controlled treatments allows the coil to be seen. Similarly, the occasional appearance of the coiled structure in untreated preparations may reflect the differential loss of this putative modifier from selected virions.

Such a mechanism could account for the inability to demonstrate the nucleoprotein in preparations of disrupted 229E while a linear structure can be demonstrated after

isolation. We have obtained micrographs suggestive of an amorphous-to-compact transition of some material in stored preparations of 229E, but the identity of the particles involved was not sufficiently clear as to constitute sound evidence.

The parallel between 229E and influenza virus may extend to the native configuration of the nucleocapsid. Figure 24B suggests that the RNP may be present as a coiled structure within the virion. The diameter of the strand we have seen is similar to that reported by Apostolov et al. (1970) on the basis of thin section studies and the arrangement we suggest is compatible with their observations. Since we are not able to obtain the more compelling evidence of a coiled structure within the virion envelope, this aspect of the viral morphology must remain conjectural.

CONCLUDING REMARKS

In this thesis, three phases of our work with the human coronavirus, 229E have been described: the development of a plaque assay system suited to our particular requirements, studies on the effect of the drug Actinomycin D on the replication of the virus and some studies on the degradation of the virus with isolation and characterization of an internal component. The subdivisions are necessarily somewhat arbitrary, as much of working with a "new" virus seems to involve the evolution of tools and techniques, and the experiences gained incidentally may be of as much value as those topics which are singled out for discussion. So too, many of the questions which arise in the context of one study may suggest the basis for future progress.

In developing the plaque assay system, it was found that DEAE-dextran and BUdR together enhanced the formation of plaques. Both of these additives have been noted to have a varied array of effects on virus-cell interactions and it would be intriguing to examine further their interactions with the 229E-L 132 system used in the present study. In the same vein, bicarbonate had a marked effect on plaque production, suggesting that a detailed examination of the effect of pH on the infectious cycle, as has been done with transmissible gastroenteritis virus (TGE, Pocock and Garwes,

1975) and infectious bronchitis virus (IBV, Alexander and Collins, 1975) might also be productive with 229E. In our additions of bicarbonate, the tonicity of the medium was not adjusted, so that at least two factors, tonicity and pH could have contributed to the effects observed. If the only result of these studies were to increase the efficiency of the infectious cycle leading to greater yields of virus, that in itself would be rewarding, as the production of adequate quantities of virus for use in antigenic studies and acrylamide gel work has been expensive in terms of time and materials.

Actinomycin D appears to specifically inhibit the synthesis of 229E in L 132 cells, affecting a reaction which seems to be of critical importance in the first third of the viral growth cycle when nucleic acid replication and the synthesis of early proteins would be taking place. Corroborating data could be obtained by studying the effects of other inhibitors known to affect RNA synthesis, or correlations might be sought between the timing of the AMD effect and the kinetics of protein and RNA synthesis as determined by a double labelling technique such as that used by Famulari and Fleisner (1976) in their study on Sendai virus. Detailed analysis of the effect, however, will have to await development of specific probes for virus products in infected cells.

In the meantime, it would be interesting to repeat the dose-response determinations in other cell lines to see

if the relationships noted between 229E, the control viruses and cellular RNA synthesis were constant or variable. The outcome of these experiments might shed light on the virus-drug relationship and/or ways in which the drug might contribute to study of the virus.

Regarding the characterization of viral components, using a gentle system of disruption, we have been able to isolate a putative nucleocapsid from 229E; moreover, this approach has allowed us to propose a model for the organization of the nucleoprotein within the virion. Several other reports have been communicated, also bearing on the structure of coronaviral particles (Almeida, in McIntosh, 1974; Garwes et al., 1976; R. W. Bingham, in press) and although no concensus has emerged, Collins et al. (1976) did report the isolation from spontaneously disrupting infectious bronchitis virus of an amorphous material somewhat similar to our isolated nucleoprotein, which they speculate to be the viral ribonucleoprotein. However, as the coronaviruses appear somewhat unpredictable in their responses to physical and chemical influences as well as being rather dissimilar in their component polypeptides (Bingham, 1975; Garwes and Pocock, 1975 and Hierholzer, 1976) minor differences in the chosen strains may well be reflected in the results obtained. Experimental conditions also varied between the three groups which may further complicate matters (e.g. note the precise disruptive conditions required for the morphological studies on influenza virus, Almeida and Brand, 1975).

Otherwise, there is the intriguing possibility that morphological subgroups might exist within the recognized coronaviruses (C. M. Johnson-Lussenburg, personal communication): how significant this difference may be and to what level of structure it may extend is at present unknown.

Whatever lies at the root of these varied findings, further work along these lines is mandatory and could profit from collaborative efforts between workers involved with the different viruses.

Work in our laboratory will continue to be directed towards physical, chemical and antigenic characterization of the virus and subviral components, including investigation of the possible presence of a virion polymerase and further studies on the mechanism of viral replication. As similar studies progress in other laboratories working on other virus-host systems and as the resulting information is exchanged, it is likely that a clearer picture of the structure and replicative pathways of the individual coronaviruses as well as their interrelationships will emerge.

REFERENCES

Ackermann, H. W.; Cherchel, G.; Valet, J. P.; Matte, J.; Moorjani, S., and Higgins, R. (1974). Expériences sur la nature de particules trouvées dans des cas d'hépatite virale: type coronavirus, antigène Australia et particules de Dane. Can. J. Microbiol. 20:193-203.

Alexander, D. J., and Collins, M. S. (1975). Effect of pH on the growth and cytopathogenicity of avian infectious bronchitis virus in chick kidney cells. Arch. Virol. 49:339-48.

Almeida, J. D., and Brand, C. M. (1975). A morphological study of the internal component of influenza virus. J. gen. Virol. 27:313-18.

Almeida, J. D.; Berry, D. M.; Cunningham, C. H.; Hamre, D.; Hofstad, M. S.; Malluci, L.; McIntosh, K., and Tyrrell, D. A. J. (1968). Coronaviruses. Nature, Lond. 220:650.

Anderson, N., and Doane, F. W. (1972). Agar diffusion method for negative staining of microbial suspensions in salt solutions. Appl. Microbiol. 24:495-96.

Anderson, N. G.; Harris, W. W.; Barber, A. A.; Rankin, C. T., jr., and Candler E. L. (1966). Separation of subcellular components and viruses by combined rate-and isopycnic-zonal centrifugation. Nat. Canc. Inst. Monog. 21:253-83.

Apostolov, K., and Flewett, T. H. (1965). Internal structure of influenza virus. Virology. 26:506-8.

Apostolov, K.; Flewett, T. H., and Kendal, A. P. 1970. Morphology of influenza A, B, C and infectious bronchitis virus (IBV) virions and their replication; in Barry and Mahy The Biology of Large RNA Viruses. Symp. Cambridge 1969, pp. 3-26. London: Academic Press.

Apostolov, K.; Spasic, P., and Bojanic, N. (1975). Evidence of a viral aetiology in endemic (Balkan) nephropathy. Lancet. ii:1271-73.

Baltimore, D. (1971). Expression of animal virus genomes. Bact. Rev. 35:235-41.

Barinsky, I. F. (1967). Species insusceptibility in viral hepatitides. Acta Virol. 11:483.

Barinsky, I. F., and Dementiev, I. V. (1968). Virological and cytogenetic studies on the involvement of the bone marrow of mice in some hepatoencephalotropic viral infections. Acta Virol. 12:464-67.

Barry, R. D., and Mahy, B. W. J. eds. (1970). The Biology of Large RNA Viruses. Symp. Cambridge 1969. London: Academic Press.

Barry, R. D.; Ives, D. R., and Cruikshank, J. G. (1962). Participation of deoxyribonucleic acid in the multiplication of influenza virus. Nature. 194:1139-40.

Berry, D. M.; Cruikshank, J. G.; Chu, H. P., and Wells, R. J. H. (1964). The structure of infectious bronchitis virus. Virology. 23:403-7.

Biedler, J. L., and Riehm, H. (1970). Cellular resistance to actinomycin D in Chinese hamster cells in vitro: cross resistance, radioautographic and cytogenetic studies. Cancer Res. 30:1174-84.

Biggart, J. D., and Ruebner, B. H. (1970). Lymphoid necrosis in the mouse spleen produced by mouse hepatitis virus (MHV 3): an electron microscopic study. J. Med. Microbiol. 3:627-32.

Bingham, R. W. (1975). The polypeptide composition of avian infectious bronchitis virus. Arch. Virol. 49:207-16.

Binn, L. N.; Lazar, E. C.; Keenan, K. P.; Huxsoll, D. L.; Marchwicki, R. H., and Strano, A. J. (1975). Recovery and characterization of a coronavirus from military dogs with diarrhea. Proc. 78th Ann Meeting, U. S. Animal Health Assoc., pp. 359-66. Roanoke, Va.: Oct. 1974.

Black, D. N., and Brown, F. (1968). The influence of mitomycin C, actinomycin D and ultraviolet light on the replication of the viruses of foot and mouth disease and vesicular stomatitis. J. gen. Virol. 3:453-57.

Bradburne, A. F., and Tyrrell, D. A. J. (1969). The propagation of coronaviruses in tissue culture. Arch. ges. Virusforsch. 28:133-50.

Bradburne, A. F., and Tyrrell, D. A. J. (1971). Coronaviruses of man. Progr. Med. Virol. 13:373-403.

Bradley, D. E. (1962). A study of the negative staining process. J. Gen. Microbiol. 29:503-16.

Brenner, S., and Horne, R. W. (1959). A negative staining method for high resolution electron microscopy of viruses. Biochim. Biophys. Acta. 34:103-10.

Bucknall, R. A.; King, L. M.; Kapikian, A. Z., and Chanock, R. M. (1972). Studies with human coronaviruses II. Some properties of strains 229E and OC43. Proc. Soc. Exp. Biol. Med. 139:722-27.

Bukrinskaya, A. G. (1973). Nucleocapsids of large RNA viruses as functionally active units in transcription. Adv. Virus Res. 18:195-255.

Campion, E. C.; Mukherjee, T. M.; Simpfendorfer, M., and Wangel, A. G. (1971). Coronavirus-like particles in human hepatitis. Aust. N.Z. J. Med. 1:275.

Caspar, D. L. D. (1965). Design principles in virus particle construction; in Horsfall, F. L. jr., and Tamm, I. eds. Viral and Rickettsial Infections of Man, pp. 51-93. Lippincott, Pa.: 1965.

Caul, E. O. and Clarke, S. K. R. (1975). Coronavirus propagated from patient with non-bacterial gastroenteritis. Lancet. ii:953-54.

Caul, E. D.; Paver, W. K., and Clarke, S. K. R. (1975). Coronavirus particles in faeces from patients with gastroenteritis. Lancet. i:1192.

Chow, N., and Simpson, R. W. (1971). RNA dependent RNA polymerase activity associated with virions and subviral particles of myxoviruses. Proc. Nat. Acad. Sci. U.S. 68:752-56.

Clarke, M. C. (1968). The effect of 5-bromodeoxyuridine and actinomycin D on the multiplication of transmissible gastroenteritis virus. J. gen. Virol. 3:267-70.

Collins, M. S.; Alexander, D. J., and Harkness, J. W. (1976). Heterogeneity of infectious bronchitis virus grown in eggs. Arch. Virol. 50:55-72.

Cooper, P. D. (1961). The plaque assay of animal viruses. Adv. Virus Res. 18:319-78.

_____. (1966). The inhibition of poliovirus growth by actinomycin D and the prevention of the inhibition by pretreatment of the cells with serum or insulin. Virology. 28:663-78.

Cooper, P. D.; Geissler, E.; Scotti, P. D., and Tannock, G. A. (1971). Further characterization of the genetic map of poliovirus temperature-sensitive mutants; in Wolstenholme, G. E. W., and O'Connor, M. eds. Strategy of the Viral Genome, pp. 75-95. London: Churchill Livingstone, 1971.

Davis, E. V., and Bolin, V. S. (1960). Continuous cultivation of isogenous cell lines from the human embryo. Fed. Proc. 19:386.

Davis, N. L., and Rueckert, R. R. (1972). Properties of a ribonucleoprotein particle isolated from Nonidet P-40-treated Rous sarcoma virus. J. Virol. 10:1010-20.

Dulbecco, R. The nature of viruses. Appendix. Quantitative aspects of infection; in Davis, B. D.; Dulbecco, R.; Ginsberg, H. S., and Wood, W. B. jr., Microbiology, 2nd ed., pp. 1042-45. Md.: Harper and Row, 1973.

Dulbecco, R. and Vogt, M. (1954). Plaque formation and isolation of pure lines with poliomyelitis virus. J. Exp. Med. 99:167-99.

Famulari, N. G., and Fleissner, E. (1976). Kinetics of utilization of Sendai virus RNA and protein in the process of virion assembly. J. Virol. 17:605-13.

Fenner, F.; McAuslan, B. R.; Mims, C. A.; Sambrook, J., and White, D. O. (1974). The Biology of Animal Viruses, pp. 319-37. New York: Academic Press.

Follett, E. A. C.; Pringle, C. R.; Wunner, W. H., and Skehel, J. J. (1974). Virus replication in enucleate cells: vesicular stomatitus virus and influenza virus. J. Virol. 13:394-99.

Fraenkel-Conrat, H., and Wagner, R. eds. (1975). Comprehensive Virology. Vol 4. Reproduction-Large RNA Viruses. New York: Plenum Press.

Garwes, D. J., and Pocock, D. H. (1975). The polypeptide structure of transmissible gastroenteritis virus. J. gen. Virol. 29:25-34.

Garwes, D. J.; Pocock, D. H., and Pike, B. V. (1976). Isolation of subviral components from TGE virus. J. gen.Virol. 32:283-94.

Garwes, D. J.; Pocock, D. H., and Wijaska, T. M. (1975). Identification of heat-dissociable RNA complexes in two porcine coronaviruses. Nature. 257:508-10.

Gregoriades, A. (1970). Actinomycin D and influenza virus multiplication in the chick embryo fibroblast. Virology. 42:905-16.

Griffith, D. M. (1975). Techniques of preparative, zonal, and continuous flow ultracentrifugation. Beckman publication "Spinco DS-468A." California: Beckman Instruments Inc.

Hamre, D., and Procknow, J. J. (1966). A new virus isolated from the human respiratory tract. Proc. Soc. Exp. Biol. Med. 121:190-93.

Hamre, D.; Kindig, D. A., and Mann, J. (1967). Growth and intracellular development of a new respiratory virus. J. Virol. 1:810-16.

Hayflick, L. (1965). The limited in vitro lifetime of human diploid cell strains. Exp. Cell Res. 37:614-36.

Hayflick, L., and Moorhead, P. S. (1961). The serial cultivation of human diploid cell strains. Exp. Cell Res. 25:585-621.

Hierholzer, J. C. (1976). Purification and biophysical properties of human coronavirus 229E. Virology. 75: 155-65.

Hirano, T., and Ruebner, B. H. (1965). The effect of murine hepatitis virus infection on lymphatic organs. Lab. Invest. 14:488-500.

Ho, M., and Armstrong, J. A. (1975). Interferon. Ann. Rev. Microbiol. 29:131-61.

Hopps, H. E.; Bernheim, B. C.; Nisalak, A.; Tjio, J. H., and Smadel, J. E. (1963). Biologic characteristics of a continuous kidney cell line derived from the African green monkey. J. Immunol. 91:416-24.

Horne, R. W. (1974). Virus Structure, p. 3. New York: Academic Press.

Horne, R. W., and Waterson, A. P. (1960). A helical structure in mumps, Newcastle disease and Sendai viruses. J. molec. Biol. 2:75-77.

Howatson, A. F. (1969). Electron microscopic procedures in virology; in Habel, K., and Salzman, N. P. eds. Fundamental Techniques in Virology, pp. 505-24. New York: Academic Press.

Howatson, A. F., and Whitmore, G. F. (1962). The development and structure of vesicular stomatitis virus. Virology. 16:466-78.

Kamen, R. (1970). Characterization of the subunits of Qβ replicase. Nature. 228:527-33.

Kapikian, A. Z.; James, H. D. jr.; Kelly, S. J., and Vaughan, A. L. (1973). Detection of coronavirus strain 692 by immune electron microscopy. Infect. Immun. 7:111-16.

Kaye, H. S.; Hierholzer, J. C., and Dowdle, W. R. (1970). Purification and further characterization of an "IBV-like" virus (coronavirus). Proc. Soc. Exp. Biol. Med. 135:457-63.

Keenan, K. P.; Jervis, H. R.; Marchwicki, R. H., and Binn, L.N. (1976). Intestinal infection of neonatal dogs with canine coronavirus 1-71: Studies by virologic, histologic, histochemical and immune fluorescent techniques. Am. J. Vet. Res. 37:247-56.

Kennedy, D. A., and Johnson-Lussenburg, C. M. (1976). Isolation and morphology of the internal component of human coronavirus, strain 229E. Intervirology. 6: 197-206.

Kondo, M.; Gallerani, R., and Weissman, C. (1970). Subunit structure of Qβ replicase. Nature. 228:525-27.

Korant, B. D., and Halperen, S. (1975). Electrophoretic analysis of capsid and non-capsid polypeptides of echovirus 12, and selective inhibition of the formation of virus particles by actinomycin D. J. gen. Virol. 26:239-48.

Lennette, E. H. (1969). General principles underlying laboratory diagnosis of viral and rickettsical infections; in Lennette, E. H., and Schmidt, N. J. eds. Diagnostic Procedures for Viral and Rickettsical Infections, pp. 47-49. New York: Am. Publ. Health Assoc., 1969.

Lomniczi, B. (1975). Metabolic requirements for the multiplication of a coronavirus: infectious bronchitis virus of fowl. Abstr. 3rd. Internat. Congr. Virology, p. 231.

Lonberg-Holm, K., and Philipson, L. (1974). Early interaction between animal viruses and cells; in Melnick, J. L. ed. Monographs in Virology, Vol. 9, pp. 95-102. Basel: S. Karger, 1974.

Loronz, R. J., and Zoeth, B. (1966). An estimation of the overlap bias in plaque assay. Virology. 28:379-85.

Lowry, O. H.; Rosebrough, N. J.; Farr, A. L., and Randall, R. J. (1951). Protein measurement with the Folin phenol reagent. J. Biol. Chem. 193:265-75.

Malluci, L. (1965). Observations on the growth of mouse hepatitis virus (MHV-3) in mouse macrophages. Virology. 25:30-37.

McEwen, C. R. (1967). Tables for estimating sedimentation through linear concentration gradients of sucrose solution. Anal. Biochem. 20:114-49.

McIntosh, K. (1974). Coronaviruses: a comparative review. Curr. Topics Microbiol. Immunol. 63:85-129.

Meienhofer, J., and Atherton, E. (1973). Structure-activity relationships in the actinomycins. Adv. Appl. Microbiol. 16:203-300.

Michel, M. R.; Hirt, B., and Weil, R. (1967). Mouse cellular DNA enclosed in polyoma viral capsids (pseudovirions). Proc. Nat. Acad. Sci. U.S. 58:1381-88.

Monto, A. S. (1974). Coronaviruses. Yale J. Biol. Med. 47: 234-41.

Newman, F. M. (1973). Beckman Biomedical Technical Report TR551. Calif: Beckman Instruments, Inc.

Nowinski, R. C.; Lloyd, J. O.; Sarkar, N. H., and Moore, D. H. (1970). Common properties of the oncogenic RNA viruses (oncornaviruses). Virology. 42:1152-57.

Parker, J. C.; Cross, S. S., and Rowe, W. P. (1970). Rat coronavirus (RCV): a prevalent, naturally occurring pneumotropic virus of rats. Arch. ges. Virusforsch. 31:293-302.

Pederson, I. B. (1971). Lymphocytic choriomeningitis virus RNAs. Nature New Biol. 234:112-14.

Perry, R. P. (1963). Selective effects of actinomycin D on the intracellular distribution of RNA synthesis in tissue culture cells. Exp. Cell Res. 29:400-406.

Pocock, D. H., and Garwes, D. J. (1975). The influence of pH on the growth and stability of TGE virus in vitro. Arch. Virol. 49:239-48.

Pons, M. W. (1973). The inhibition of influenza virus RNA synthesis by actinomycin D and cycloheximide. Virology. 51:120-28.

Prince, A. M.; Brotman, B.; Grady, G. F.; Kuhns, W. J.; Hazzi, C.; Levine, R. W., and Millian, S. J. (1974). Long incubation post-transfusion hepatitis without serological evidence of exposure to hepatitis B virus. Lancet. ii:241-46.

Reich, E., and Goldberg, I. H. (1964). Actinomycin and nucleic acid function. Progr. Nucl. Acid. Res. 3:183-234.

Reich, E.; Franklin, R. M.; Shatkin, A. J., and Tatum, E. L. (1961). Effect of actinomycin D on cellular nucleic acid synthesis and virus production. Science. 134:556-7.

Reich, E.; Franklin, R. M.; Shatkin, A. J., and Tatum, E. L. (1962). Action of actinomycin D on animal cells and viruses. Proc. Nat. Acad. Sci. U.S. 48:1238-45.

Reid, D. B. W. (1968). Statistical methods in virology; in Rhodes, A. J., and Van Rooyen, C. E., eds. Textbook of Virology, 5th ed., pp. 104-24. Baltimore: Williams and Wilkins, 1968.

Robinson, W. S. (1971). Ribonucleic acid polymerase activity in Sendai virions and nucleocapsid. J. Virol. 8:81-86.

Rossier, E., and Landry-Pigeon, D. (1972). Large scale production of peripheral human lymphocytes for viral studies: the influence of viability and P.H.A. transformation on the growth of vesicular stomatitis virus. Can. J. Microbiol. 18:465-91.

Sawicki, S. G., and Godman, G. C. (1972). On the recovery of transcription after inhibition by actinomycin D. J. Cell Biol. 55:299-309.

Schmidt, N. J. (1969). Tissue culture techniques for diagnostic virology; in Lennette, E. H., and Schmidt, N. J. eds., Diagnostic Procedures for Viral and Rickettsial Infections, 4th ed., pp. 79-178. New York: A.P.H.A.

Shannon, J. E., and Macy, M. L. (1972). Registry of Animal Cell Lines, 2nd ed. Maryland: American Type Culture Collection.

Sharpee, R., and Mebus, C. A. (1975). Rotaviruses of man and animals. Lancet. i:639.

Siegel, A. (1971). Pseudovirions of tobacco mosaic virus. Virology. 46:50-59.

Simpson, R. W., and Hauser, R. E. (1966). Structural components of vesicular stomatitis virus. Virology. 29:654-67.

Snedecor, G. W., and Cochran, W. G. Statistical Methods, 6th ed. Iowa: Iowa State University Press, 1967.

Szilagyi, J. F., and Uryvayev, L. (1973). Isolation of an infectious ribonucleoprotein from vesicular stomatitis virus containing an active RNA transcriptase. J. Virol. 11:279-86.

Tannock, G. A. (1973). The nucleic acid of infectious bronchitis virus. Arch. ges. Virusforsch. 43:259-71.

Tyrrell, D. A. J.; Almeida, J. D.; Cunningham, C. H.; Dowdle, W. R.; Hopstad, M. S.; McIntosh, K.; Tajima, M.; Zakstelskaya, L. Ya.; Easterday, B. C.; Kapikian, A., and Bingham, R. W. (1975). Coronaviridae. Intervirology. 5:76-82.

Valle, M. (1971). Factors affecting plaque assay of animal viruses. Acta Path. Microbiol. Scand. B. Supp. 219.

Wallis, C., and Melnick, J. L. (1962). Magnesium chloride enhancement of cell susceptibility to poliovirus. Virology. 16:122-32.

Watkins, H., Reeve, P., and Alexander, D. J. (1975). The ribonucleic acid of infectious bronchitis virus. Arch. Virol. 47:279-86.

Wigand, R., and Schmieder, J. (1973). Inhibition of adenovirus multiplication by metabolic inhibitors. Arch. ges. Virusforsch. 42:324-38.

Wiktor, T. J., and Koprowski, H. (1974). Rhabdovirus replication in enucleated host cells. J. Virol. 14:300-306.

Witte, K. H.; Tajima, M., and Easterday, B. C. (1968). Morphologic characteristics and nucleic acid type of transmissible gastroenteritis virus of pigs. Arch. ges. Virusforsch. 23:53-70.

Yamazaki, S., and Notkins, A. L. (1973). Inhibition of replication of lactic dehydrogenase virus by actinomycin. J. Virol. 11:473-78.

Zuckerman, A. J.; Taylor, P. E., and Almeida, J.D. (1970). Presence of particles other than the Australia-SH antigen in a case of chronic active hepatitis with cirrhosis. Brit. Med. J. 1:262-64.

ABSTRACT

This thesis describes three phases of our studies on the biology of human coronavirus, 229E: the development of a plaque assay system, studies on the effect of Actinomycin D on the replication of this virus, and the isolation and preliminary characterization of an internal component of the virion.

A medium was developed which permitted the production of plaques by 229E on monolayers of L 132 cells in closed containers which could be incubated in regular incubators, a result which we were not able to duplicate using published formulations. This assay system exhibited a linear dose-response curve over a wide range of virus concentrations and was applicable to the assay of this virus in several cell lines; in addition, it could be used for the assay of other viruses. Several other features of the assay are also discussed briefly.

The replication of 229E in L 132 cells was found to be inhibited in the presence of Actinomycin D, a potent inhibitor of DNA-dependent RNA synthesis. While the drug has adverse effects on the host cell, several arguments have been brought forth which argue in favor of a specific effect on virus replication; the replication of vesicular stomatitis virus was unimpeded at 10 times the 50% inhibitory level of

AMD for 229E, and largely unaffected at 100 times the mean inhibitory dose; in addition the cells were not themselves greatly affected and the time course of drug sensitivity appeared to indicate a temporally discrete period of AMD susceptibility. The sensitivity of AMD was shown to be dependent on the virus input used to initiate the replicative cycle.

Using disruption by the detergent Nonidet P-40, we were able to isolate, in sucrose gradients, a subviral particle. This particle, a nucleoprotein, has a density of 1.27 and appears linear in the electron microscope. It is suggested that this structure probably represents the viral nucleocapsid. Some further aspects of its relation to virus morphology are discussed.